Atmos. Chem. Phys. Discuss., doi:10.5194/acp-2016-924, 2016
Manuscript under review for journal Atmos. Chem. Phys.
Published: 31 October 2016

Multi-model study of mercury dispersion in the atmosphere: Atmospheric processes and model evaluation

Oleg Travnikov[1], Hélène Angot[2], Paulo Artaxo[3], Mariantonia Bencardino[4], Johannes Bieser[5], Francesco D'Amore[4], Ashu Dastoor[6], Francesco De Simone[4], María del Carmen Diéguez[7], Aurélien Dommergue[2,8], Ralf Ebinghaus[5], Xin Bin Feng[9], Christian N. Gencarelli[4], Ian M. Hedgecock[4], Olivier Magand[8], Lynwill Martin[10], Volker Matthias[5], Nikolay Mashyanov[11], Nicola Pirrone[12], Ramesh Ramachandran[13], Katie Alana Read[14], Andrei Ryjkov[6], Noelle E. Selin[15,16], Fabrizio Sena[17], Shaojie Song[15], Francesca Sprovieri[4], Dennis Wip[18], Ingvar Wängberg[19], and Xin Yang[20]

[1]Meteorological Synthesizing Centre – East of EMEP, Moscow, Russia
[2]University Grenoble Alpes, Laboratoire de Glaciologie et Géophysique de l'Environnement, Grenoble, France
[3]University of Sao Paulo, Sao Paulo, Brazil
[4]CNR Institute of Atmospheric Pollution Research, Rende, Italy
[5]Institute of Coastal Research, Helmholtz-Zentrum Geesthacht, Geesthacht, Germany
[6]Air Quality Research Division, Environment and Climate Change Canada, Canada
[7]INIBIOMA-CONICET-UNComa, Bariloche, Argentina
[8]CNRS, Laboratoire de Glaciologie et Géophysique de l'Environnement, Grenoble, France
[9]Institute of Geochemistry, State Key Laboratory of Environmental Geochemistry, Chinese Academy of Sciences, Guiyang, China
[10]Cape Point GAW Station, Climate and Environment Research & Monitoring, South African Weather Service, Stellenbosch, South Africa
[11]St. Petersburg State University, St. Petersburg, Russia
[12]CNR Institute of Atmospheric Pollution Research, Rome, Italy
[13]Institute for Ocean Management, Anna University, Chennai, India
[14]NCAS, University of York, York, UK
[15]Department of Earth, Atmospheric and Planetary Sciences, Massachusetts Institute of Technology, Cambridge, MA, USA
[16]Institute for Data, Systems, and Society, Massachusetts Institute of Technology, Cambridge, MA, USA
[17]Joint Research Centre, Ispra, Italy
[18]Department of Physics, University of Suriname, Paramaribo, Suriname
[19]IVL, Swedish Environmental Research Inst. Ltd., Göteborg, Sweden
[20]British Antarctic Survey, Cambridge, United Kingdom

Correspondence to: O. Travnikov (oleg.travnikov@msceast.org)

Abstract.

Current understanding of mercury (Hg) behaviour in the atmosphere contains significant gaps. Some key characteristics of Hg processes including anthropogenic and geogenic emissions, atmospheric chemistry, and air-surface exchange are still poorly known. This study provides a complex analysis of processes governing Hg fate in the atmosphere involving both measurement data from ground-based sites and simulation results of chemical transport models. A variety of long-term measurements of gaseous elemental Hg (GEM) and reactive Hg (RM) concentration as well as Hg wet deposition flux has been compiled from different global and regional monitoring networks. Four contemporary global-scale transport models for Hg were applied both in their state-of-the-art configurations and for a number of numerical experiments aimed at evaluation of particular processes.

Atmos. Chem. Phys. Discuss., doi:10.5194/acp-2016-924, 2016
Manuscript under review for journal Atmos. Chem. Phys.
Published: 31 October 2016

Results of the model simulation were evaluated against measurements. As it follows from the analysis the inter-hemispheric gradient of GEM is largely formed by the spatial distribution of anthropogenic emissions which prevail in the Northern Hemisphere. Contribution of natural and secondary emissions enhances the south-to-north gradient but their effect is less significant. The atmospheric chemistry does not affect considerably both spatial distribution and temporal variation of GEM concentration in the surface air. On the other hand, RM air concentration and wet deposition are largely defined by oxidation chemistry. The Br oxidation mechanism allows successfully reproducing observed seasonal variation of the RM/GEM ratio in the near-surface layer, whereas it predicts maximum in wet deposition in spring instead of summer as observed at monitoring sites located in North America and Europe. Model runs with the OH chemistry correctly simulate both the periods of maximum and minimum values and the amplitude of observed seasonal variation but lead to shifting the maximum RM/GEM ratios from spring to summer. The O_3 chemistry does not provide significant seasonal variation of Hg oxidation. Thus, performance of the considered Hg oxidation mechanisms differs in reproduction of different observed parameters that can imply possibility of more complex chemistry and multiple pathways of Hg oxidation occurring concurrently in various parts of the atmosphere.

1 Introduction

Mercury (Hg) is widely recognised as a toxic pollutant capable of long-range transport, bioaccumulation in ecosystems and biota as well as adverse effects on human health and the environment. In spite of being a natural element its concentrations in the environment has been considerably enriched by human activities since the pre-industrial times (Fitzgerald et al., 1998; Mason and and Sheu, 2002; Krabbenhoft and Sunderland, 2013). Once emitted to the atmosphere Hg can be dispersed globally impacting remote regions through deposition to aquatic ecosystems, transformation to a potent neurotoxic form (methylmercury), and bioaccumulation in food chains (Mahaffey et al., 2004; Sunderland et al., 2010; Mason et al., 2012). The character of Hg transport and fate in the atmosphere is largely determined by properties of its chemical forms. Mercury is emitted into the atmosphere from anthropogenic sources in a form of both gaseous elemental mercury (GEM) and Hg oxidized chemical compounds (Pirrone et al., 2010). The latter are typically divided into two operationally defined forms – gaseous oxidized mercury (GOM) and particle bound mercury (PBM). In addition, GEM can also originate from natural geogenic and secondary sources (Mason, 2009). Reactive mercury (RM = GOM + PBM) can also be produced in the atmosphere from gas- and aqueous-phase oxidation of GEM (Lindberg and Stratton, 1998). Relatively stable and slightly soluble GEM can drift in the atmosphere for months providing transport of Hg mass over the globe (Schroeder and Munthe, 1998). In contrast, RM is easily removed from the air by precipitation scavenging (wet deposition) or surface uptake (dry deposition) (Schroeder and Munthe, 1998; Gustin et al., 2012; Sather et al., 2013; Wright et al., 2014). GEM can also contribute to Hg dry deposition through air-surface exchange with various terrestrial and aquatic compartments (Zhang et al., 2009; Wang et al., 2014, 2016). On the other hand, previously deposited Hg may be reduced to the elemental form and re-emitted back to the atmosphere (Gustin, 2012; Qureshi et al., 2012).

Atmospheric redox chemistry plays an important role in Hg long-range dispersion and deposition. However, particular mechanisms of Hg oxidation in the atmosphere are not well understood (Lin et al., 2006; Subir et al., 2011, ?; Gustin et al., 2015; Ariya et al., 2015). Gaseous reactive halogens, in particular atomic Br, are believed to play a major role in the atmospheric

Atmos. Chem. Phys. Discuss., doi:10.5194/acp-2016-924, 2016
Manuscript under review for journal Atmos. Chem. Phys.
Published: 31 October 2016

oxidation of GEM (Goodsite et al., 2004, 2012; Donohoue et al., 2006; Hynes et al., 2009). There exists observational evidence that the Br-initiated chemistry is a dominant GEM oxidation pathway in some atmospheric environments including the marine boundary layer, the polar regions, and the upper troposphere/lower stratosphere (Hedgecock and Pirrone, 2004; Holmes et al., 2009; Lyman and Jaffe, 2010; Obrist et al., 2011; Gratz et al., 2015). However, very limited data exists with respect to this mechanism in the global atmosphere (Kos et al., 2013). Nevertheless, application of the Br chemistry as the only oxidation pathway in a chemical transport model allows simulation of Hg atmospheric cycle and reproduction of available observations (Holmes et al., 2010; Soerensen et al., 2010; Amos et al., 2012; Shah et al., 2016). On the other hand, in spite of theoretical doubts of viability and significance of direct GEM oxidation by O_3 and OH radical under atmospheric conditions (**?**Hynes et al., 2009), numerous modelling works applying these reactions as the main pathways of GEM oxidation in the free troposphere also demonstrate reasonable results in terms of comparison with observed GEM concentration and wet deposition flux (Christensen et al., 2004; Travnikov and Ilyin, 2009; Pan et al., 2010; Baker et al., 2012; Kos et al., 2013; Gencarelli et al., 2014; De Simone et al., 2015; Cohen et al., 2016). Besides, both theoretical and laboratory studies suggest that complex Hg oxidation mechanisms involving O_3 and OH can exist in the atmosphere in presence of aerosol particles and secondary reactants (Snider et al., 2008; Cremer et al., 2008; Rutter et al., 2012; Subir et al., 2011; Ariya et al., 2015). It is interesting to note that recent comparison studies showed that models with diverse formulations of atmospheric chemistry agree well when simulated Hg transport on a global scale and source attribution of Hg deposition (Travnikov et al., 2010; AMAP/UNEP, 2013a, 2015).

Application of chemical transport models complimented by extensive measurement data can facilitate a better understanding of the principal mechanisms governing Hg dispersion and cycling in the atmosphere. Effect of atmospheric redox chemistry as well as anthropogenic and natural emissions on the fate of atmospheric Hg were investigated systematically in a number of earlier modelling studies (Seigneur et al., 2006; Seigneur and Lohman, 2008; Lohman et al., 2008). In more recent work Kos et al. (2013) performed a detailed analysis of uncertainties associated with RM measurements and modelling. A number of model sensitivity runs were carried out to evaluate different chemical mechanisms and speciation of anthropogenic emissions of Hg. In particular, they found evident inconsistency between the emission speciation in the existing emission inventories with measured RM concentration in the surface air. Weiss-Penzias et al. (2015) applied a global-scale model for Hg to analyse speciated atmospheric Hg measurements from five high and mid-elevation sites. The results of the study suggested the presence of different chemical regimes in different parts of the troposphere and signals that there is not necessarily one single global oxidant. Shah et al. (2016) used the same chemical transport model to interpret aircraft measurements of RM and place new constraints on Br-initiated chemistry in the free troposphere. They found that the standard model simulations significantly underestimate observed RM and that modelling with tripled Br concentrations or a faster oxidation rate constant can improve agreement with observations. A detailed process-specific atmospheric lifetime analysis was carried out by Cohen et al. (2016) providing important insights into the fate and transport of atmospheric Hg as well as total Hg deposition to the Great Lakes. A global-scale chemical transport model has also been applied by Song et al. (2015) for inverse modelling aimed at constraining present-day atmospheric Hg emissions and relevant physiochemical parameters.

Atmos. Chem. Phys. Discuss., doi:10.5194/acp-2016-924, 2016
Manuscript under review for journal Atmos. Chem. Phys.
Published: 31 October 2016

In the current study we apply four contemporary global-scale Hg chemical transport models in combination with a variety of long-term measurements of Hg concentration and wet deposition from different monitoring networks to analyse processes governing Hg fate in the atmosphere. A number of numerical experiments aimed at evaluation of effect of anthropogenic and natural/secondary emissions as well as different chemical oxidation mechanisms on levels and spatio-temporal variation of GEM and RM air concentration and Hg wet deposition. The study was performed as part of the Mercury Modelling Task Force (MMTF), a scientific cooperative initiative under the EU funded project "Global Mercury Observation System" (GMOS, www.gmos.eu).

2 Methods

2.1 Measurements

A variety of measurement data was used for evaluation of the model experiments. The measurement dataset is based on the global GMOS monitoring network for Hg (Sprovieri et al., 2016a, b; GMOS, 2016) complimented with data from the EMEP regional network for Europe (Tørseth et al., 2012; EMEP, 2016) and data from the NADP/MDN (Prestbo and Gay, 2009; NADP/MDN, 2016), AMNet (Gay et al., 2013; AMNet, 2016) and NAtChem (Cole et al., 2013; Steffen et al., 2015; NAtChem, 2016) networks for North America. We compiled available measurements of GEM, GOM and PBM concentration in air as well as wet deposition flux performed at ground-based sites in 2013. At the majority sites of interest the unspeciated measurements of atmospheric Hg are performed as GEM (Gay et al., 2013; Sprovieri et al., 2016a; Angot et al., 2016). However, there is still no complete scientific evidence on whether GEM or TGM concentration is measured at some particular sites since it largely depends on local ambient conditions and configuration of the measurement setup (Gustin et al., 2015; Slemr et al., 2015). Nevertheless, as the difference between long-term observations of GEM and TGM commonly does not exceed a few percents (Slemr et al., 2015) we interpret all the unspeciated Hg measurements as GEM. Measured values of RM are used in the study instead of observations of individual species GOM and PBM. RM appears to be more valuable for the analysis since measurements of the individual species are associated with higher uncertainties (Gustin et al., 2015; Weiss-Penzias et al., 2015). Therefore, only sites with co-located observations of GOM and PBM are use in the study.

The original measurement data with high temporal resolution were processed to get monthly and yearly mean values. According to the accepted criteria monthly averages are used for the analysis if the original data cover at least 15 days of the month. Monthly averages are used both for generation of yearly mean values and for characterizing the seasonal variation of the observed parameter. In both cases only sites with temporal coverage of at least 7 months are selected. Characteristics of the selected sites measuring GEM, RM and wet deposition are given in Tables S1, S2 and S3 in the Supplement, respectively. Geographical location of the whole collection of sites is shown in Fig. 1. In total, the dataset includes 49 sites measuring GEM, 14 sites measuring RM, and 124 sites measuring wet deposition. Observations of GEM are relatively uniformly distribution over the globe with somewhat higher density in the Northern Hemisphere. In contrast, RM is mostly observed in the northern

Atmos. Chem. Phys. Discuss., doi:10.5194/acp-2016-924, 2016
Manuscript under review for journal Atmos. Chem. Phys.
Published: 31 October 2016

temperate latitudes. There are only few sites located in the Tropics and further southward. The majority of wet deposition measurements are located in North America and Europe limiting possibility of model evaluation in other regions.

2.2 Models

The model ensemble of the study includes four chemical transport models simulating mercury on a global scale (Table table:models). The models differ considerably in general formulation, spatial resolution, and applied parameterizations of physical and chemical processes. Horizontal spatial resolution of the models ranges from 1 to 2.8 degrees in latitude and longitude. The upper boundaries of the model domains vary from 10 hPa (~ 30 km) to 0.01 hPa (~ 80 km). Two of the models (GLEMOS, GEOS-Chem) utilize off-line meteorological data prepared by external pre-processor, whereas the two others (GEM-MACH-Hg and ECHMERIT) generate the meteorological fields along with simulation of the pollutant transport. All the models used the same dataset of Hg anthropogenic emissions (AMAP/UNEP, 2013a, b) with somewhat different speciation of mercury forms applied in the BASE case. In contrast, parameterizations of natural and secondary emissions significantly differ among the models. The major chemical mechanisms applied in the standard model configuration that used in the BASE case are also essentially different. The base-case reactions of GLEMOS and ECHMERIT include Hg oxidation by ozone and OH radical. The chemical scheme of GEM-MACH-Hg is base on the reaction with OH radical with application of the Br chemistry in the Polar regions. GEOS-Chem considers the Br chemistry as the only pathway of Hg oxidation in the gas phase. Besides, two of four models (GLEMOS and ECHMERIT) also include the Hg redox chemistry in the aqueous phase in cloud water. More detailed description of the model parameterisations is given below.

2.2.1 GLEMOS

GLEMOS (Global EMEP Multi-media Modelling System) is a multi-scale chemical transport model developed for the simulation of environmental dispersion and cycling of different chemicals including mercury based on the older hemispheric model MSCE-HM-Hem (Travnikov, 2005; Travnikov and Ilyin, 2009; Travnikov et al., 2009). The model simulates atmospheric transport, chemical transformations and deposition of three Hg species (GEM, GOM and PBM). The atmospheric transport of the tracers is driven by meteorological fields generated by the Weather Research and Forecast modelling system (WRF) (Skamarock et al., 2007) fed by the operational analysis data from the European Centre for Medium-Range Weather Forecasts (ECMWF) (ECMWF, 2016). In the base configuration the model grid has a horizontal resolution $1^\circ \times 1^\circ$. Vertically, the model domain reaches 10 hPa and consists of 20 irregular terrain-following sigma layers. The atmospheric chemical scheme includes Hg oxidation and reduction chemical reactions in both the gaseous and aqueous phase of cloud water. The major chemical mechanisms in the gas phase include Hg oxidation by O_3 and OH radical with the rate constants of reactions from Hall (1995) and Sommar et al. (2001), respectively. The latter was scaled down by a factor 0.1 in the cloud environment and below clouds to account for reduction of photochemical activity (Seigneur et al., 2001). The O_3 and OH concentration fields are imported from MOZART (Emmons et al., 2010). A two-step gas-phase oxidation of GEM by Br is included optionally. Aqueous-phase reactions include oxidation by ozone, chlorine and hydroxyl radical and reduction via decomposition of sulphite complexes Van Loon et al. (2000). The model distinguishes in-cloud and sub-cloud wet deposition of PBM and GOM based on empirical

Atmos. Chem. Phys. Discuss., doi:10.5194/acp-2016-924, 2016
Manuscript under review for journal Atmos. Chem. Phys.
Published: 31 October 2016

data. The dry deposition scheme is based on the resistance analogy approach (Wesely and Hicks, 2000). Prescribed fluxes of Hg natural and secondary emissions from soil and seawater were generated depending on Hg concentration in soil, soil temperature and solar radiation for emissions from land and proportional to the primary production of organic carbon in seawater for emissions from the ocean (Travnikov and Ilyin, 2009). In addition, an empirical parameterization of the prompt Hg re-emission from snow- and ice-covered surfaces is applied based on the observational data.

2.2.2 GEOS-Chem

The GEOS-Chem global chemical transport model (v9-02; www.geos-chem.org) is driven by assimilated meteorological data from the NASA GMAO Goddard Earth Observing System (Bey et al., 2001). The GEOS-FP and GEOS-5.2.0 data are used for the simulation year of 2013 and the spin-up period, respectively (http://gmao.gsfc.nasa.gov/products/). GEOS-Chem couples a 3-D atmosphere (Holmes et al., 2010), a 2-D mixed layer slab ocean (Soerensen et al., 2010), and a 2-D terrestrial reservoir (Selin et al., 2008) in a horizontal resolution of $2° \times 2.5°$. Three mercury tracers (GEM, GOM, and PBM) are tracked in the atmosphere (Amos et al., 2012). A two-step gaseous oxidation mechanism initialized by Br atoms is used. Br fields are archived from a full-chemistry GEOS-Chem simulation (Parrella et al., 2012) while the rate constants of reactions are from Goodsite et al. (2012), Donohoue et al. (2006), and Balabanov et al. (2005). The surface fluxes of GEM include anthropogenic sources, biomass burning, geogenic activities, as well as the bidirectional fluxes in the atmosphere-terrestrial and atmosphere-ocean exchanges (Song et al., 2015). Biomass burning emissions are estimated using a global CO emission database and a volume ratio of Hg/CO of 1×10^{-7}. Geogenic activities are spatially distributed based on the locations of mercury mines. For atmosphere-terrestrial exchange, GEOS-Chem treats the evasion and dry deposition of GEM separately (Selin et al., 2008). Dry deposition is parameterized with a resistance-in-series scheme (Wesely, 1989). Besides, an effective GOM uptake by sea-salt aerosol is also included over the ocean (Holmes et al., 2010). GEM evasion includes volatilization from soil and rapid recycling of newly deposited Hg. The former is estimated as a function of soil Hg content and solar radiation. The latter is modeled by recycling a fraction of wet/dry deposited RM to the atmosphere as GEM immediately after deposition (60% for snow covered land and 20% for all other land uses) (Selin et al., 2008). GEOS-Chem estimates the atmosphere-ocean exchange of GEM using a standard two-layer diffusion model. The ocean mercury in the mixed layer interacts not only with the atmospheric boundary layer but also with the subsurface waters through entrainment/detrainment of the mixed layer and wind-driven Ekman pumping (Soerensen et al., 2010).

2.2.3 GEM-MACH-Hg

GEM-MACH-Hg is a new chemical transport model for mercury that is based on the GRAHM model developed by Environment and Climate Change Canada (Dastoor04,Dastoor08,Durnford10,Durnford12,Kos13,Dastoor15). GEM-MACH-Hg uses a newer version of the Environment and Climate Change Canada's operational meteorological model. The horizontal resolution of the model is $1° \times 1°$. GEM is oxidized in the atmosphere by OH radical. The rate constant of the reaction is from Sommar et al. (2001), but scaled down by a coefficient of 0.34 to take into account possible dissociation/reduction reactions (Tossell et al., 2003; Goodsite et al., 2004). The gaseous oxidation of mercury by bromine is applied in the polar regions using

Atmos. Chem. Phys. Discuss., doi:10.5194/acp-2016-924, 2016
Manuscript under review for journal Atmos. Chem. Phys.
Published: 31 October 2016

Atmospheric Chemistry and Physics Discussions

reaction rate constants from Donohoue et al. (2006), Dibble et al. (2012) and Goodsite et al. (2004). The parameterization of AMDEs is based on Br production and chemistry, and snow re-emission of GEM (Dastoor et al., 2008). OH fields are from MOZART (Emmons et al., 2010) while BrO is derived from 2007-2009 satellite observations of BrO vertical columns. The associated Br concentration is then calculated from photochemical steady state (Platt and Janssen, 1995). Dry deposition in GEM-MACH-Hg is based on the resistance approach (Zhang, 2001; Zhang et al., 2003). In the wet deposition scheme, GEM and GOM are partitioned between cloud droplets and air using a temperature-dependent Henry's law constant. Total global emissions from natural sources and re-emissions of previously deposited Hg (from land and oceans) in GEM-MACH-Hg are based on the global Hg budgets by Gbor et al. (2007), Shetty et al. (2008) and Mason (2009). Land-based natural emissions are spatially distributed according to the natural enrichment of Hg. Land re-emissions are spatially distributed according to the historic deposition of Hg and land-use type and depend on solar radiation and the leaf area index. Oceanic emissions depend on the distributions of primary production and atmospheric deposition.

2.2.4 ECHMERIT

ECHMERIT is a global on-line chemical transport model, derived on the ECHAM5 global circulation model, with a highly flexible chemistry mechanism designed to facilitate the investigation of atmospheric mercury chemistry (Jung et al., 2009; De Simone et al., 2014, 2015, 2016). The model uses the same spectral grid of ECHAM. The standard horizontal resolution of the model is T42 (approximately, $2.8° \times 2.8°$), whereas in the vertical the model is discretized with a hybrid-sigma pressure system with non-equidistant levels up to 10 hPa. The base chemical mechanism includes the GEM oxidation by OH and O_3 in the gaseous and aqueous phases. Reaction rate constants are from Sommar et al. (2001), Hall (1995), and Munthe (1992), respectively. OH and O_3 concentration fields were imported from MOZART (Emmons et al., 2010). The Hg oxidation by Br is also optionally available by a two-step gas phase oxidation mechanism with reaction rates as described in Goodsite et al. (2004), Goodsite et al. (2012) and Donohoue et al. (2006). ECHMERIT applied parameterisation of dynamic air-seawater exchange as a function of ambient parameters but using a constant value of mercury concentration in seawater (De Simone et al., 2014). Emissions from soils and vegetation were calculated off-line and derived from the EDGAR/POET emission inventory (Granier et al., 2005; Peters and Olivier, 2003) that includes biogenic emissions from the GEIA inventories (http://www.geiacenter.org), as described by Jung et al. (2009). Prompt re-emission of a fixed fraction (20%) of wet and dry deposited mercury is applied in the model to account for reduction and evasion processes which govern mercury short-term cycling between the atmosphere and terrestrial reservoirs (Selin et al., 2008). This fraction is increased to 60% for snow-covered land and the ice covered seas.

2.3 Emissions data

The global inventory of Hg anthropogenic emissions for 2010 (AMAP/UNEP, 2013a, b) was used in the study. The original dataset consists of gridded emission data with spatial resolution $0.5° \times 0.5°$ for three Hg species (GEM, GOM, and PBM). Total global emissions of mercury from anthropogenic sources are estimated at 1875 tonnes per year with the overall share of GEM, GOM, and PBM emissions equal to 81%, 15%, and 4%, respectively. As it was mentioned above some models modified the original speciation of anthropogenic emissions (Table 1) in the BASE case simulation. No information on temporal variation

Atmos. Chem. Phys. Discuss., doi:10.5194/acp-2016-924, 2016
Manuscript under review for journal Atmos. Chem. Phys.
Published: 31 October 2016

of emissions is available in the dataset. Geographically, significant Hg emissions are predicted in industrial regions of East and South Asia, Central Europe and the eastern part of North America (Fig. S1 in the Supplement). Besides, high emission fluxes are characteristics of some areas of Central and South America, Sub-Saharan Africa and Southeast Asia due to mercury releases from the artisanal and small-scale gold mining. Almost no emissions are predicted in the Arctic and Antarctic regions.

2.4 Model experiments

The study was organized in a form of multiple model experiments aimed at evaluation of particular processes and mechanisms of Hg atmospheric chemistry as well as anthropogenic and natural/secondary emissions. A summary of the model experiments is given Table 2. All the models performed the BASE case simulation representing the state-of-the-art model configuration and is used as a reference point for other model experiments. All the models use the same anthropogenic emissions but applying the model specific speciation (see Secion 2.3). The NoANT run is based on the same standard model configuration but is carried out with the turned off anthropogenic emissions. Since Hg emissions from natural and secondary sources are fully or partly represented in the models as bi-directional air-surface exchange flux or as re-emission of previously deposited Hg (Table 1) simple exclusion of this emission type from simulations is not feasible without disturbance of the whole Hg cycle in the model. On the other hand, assuming additivity of Hg processes in the atmosphere with respect to contribution of different sources the effect of natural/secondary emissions (NoNAT) can be estimated by subtraction of NoANT results from the BASE case. Four additional model experiments are aimed at evaluation of different chemical mechanisms of GEM oxidation in the atmosphere. To avoid influence of direct anthropogenic emissions on simulated RM concentrations all emissions are assumed to be in a form of GEM. The model runs BrCHEM1 and BrCHEM2 include the only mechanism of GEM oxidation by atomic Br but utilizing two different datasets of Br concentration in the atmosphere: simulated by the GEOS-Chem (Parrella et al., 2012) and p-TOMCAT (Yang et al., 2005, 2010) models. Comparison of spatial and temporal variation of Br concentration from these two datasets is given in Figs. S6 and S9 in the Supplement. Two other experiments O3CHEM and OHCHEM are based on application of O_3- and OH-initiated oxidation chemistry. The models utilized the same datasets of O_3 and OH concentrations extracted from simulations results of the MOZART model (Emmons et al., 2010). Spatial gradients and seasonal variation of the reactants are shown in Figs. S7-S8 and S10-S11 in the Supplement, respectively. It should be noticed that not all of the models performed the whole simulations program. Results of the study are presented below bases on available simulations for each particular experiment.

2.5 Statistical analysis

Comparison of modelling results with observations are performed using the following statistical parameters. Both spatial and temporal correlation of simulated and observed values is characterised by the Pearson correlation coefficient:

$$R_{corr} = \frac{\sum_i (M_i - \overline{M})(O_i - \overline{O})}{\sqrt{\sum_i (M_i - \overline{M})^2 \sum_i (O_i - \overline{O})^2}}\,, \qquad (1)$$

where M_i and O_i are are monthly or annual mean simulated and observed values, respectively. $\overline{M}$ and $\overline{O}$ are average values. The averaging and summing are performed over monthly values for calculation of temporal correlation at particular site or

Atmos. Chem. Phys. Discuss., doi:10.5194/acp-2016-924, 2016
Manuscript under review for journal Atmos. Chem. Phys.
Published: 31 October 2016

over annual mean values of all the sites for calculation of the spatial correlation coefficient. An arithmetic mean of all temporal correlation coefficients for individual sites is then used in the analysis. Discrepancy between simulated and observed values is characterized by a symmetric relative bias:

$$\mathrm{RBIAS} = 2\,\frac{\overline{M}-\overline{O}}{\overline{M}+\overline{O}}\,100\% \,. \qquad (2)$$

RBIAS varies within the range $\pm 200\%$, and small deviations between model results and observations are characterized by values that are close to zero.

3 Results and discussion

3.1 Gaseous elemental mercury

Concentration of GEM in air is a parameter representing the balance between Hg global emissions and sinks via chemical transformation to other Hg forms or direct interaction with the surface. Given GEM long residence time in the atmosphere its spatio-temporal gradients likely characterize distribution of global emission regions as well as long-range atmospheric dispersion and cycling in the atmosphere (Selin, 2009; Travnikov, 2012; Ariya et al., 2015). Figure 2 shows global distributions of GEM concentration in the surface air simulated by four global models according to the BASE case along with ground-based observations presented by coloured circles in the same colour palette. The models predict similar spatial patterns of Hg concentration with pronounced gradient between the Southern Hemisphere (ca. 0.9-1.1 $\mathrm{ng\,m^{-3}}$) and the Northern Hemispheres (ca. 1.1-1.6 $\mathrm{ng\,m^{-3}}$) and elevated concentrations in the major industrial regions – East and South Asia, Europe and North America (above 1.4 $\mathrm{ng\,m^{-3}}$). Elevated concentrations are also predicted in tropical areas of South America, Central Africa and Southeast Asia, where considerable Hg emissions from the artisanal and small-scale gold mining are expected (AMAP/UNEP, 2013a). The models generally agree with ground-based observations shown in Fig. 2. The measurements also demonstrate evidence of the statistically significant inter-hemispheric gradient and relatively high concentrations in industrial regions (Sprovieri et al., 2016a). More detailed comparison of the modelling results with measurements is given in Fig. S2 in the Supplement. The model-measurement divergence does not commonly exceed $\pm 30\%$. In general, the models demonstrate lower spatial variation of annual GEM concentration than the measurements do. This can be partly explained by relatively low spatial resolution of the model grids (1-3 hundreds of kilometres) that can hardly allow them to reproduce local meteorological conditions at measurement sites.

It should be noticed that the models predict similar global spatial patterns of GEM concentration in spite of significant deviations in applied parameterizations of physical and chemical processes. As it was mentioned in Section 2.2 the models in their base configurations apply quite different chemical mechanisms of GEM oxidation in the atmosphere. Besides, even utilizing the same anthropogenic emissions data they largely differ in their estimates of natural and secondary emissions and Hg air-surface exchange. Higher oxidative capacity of the atmospheric chemistry leads to shorter residence time of GEM in the atmosphere and ultimately to larger deposition to the ground, which, in its turn, can be compensated by more intensive natural or re-emission to the atmosphere. Thus, combination of these compensative factors allows simulation of realistic GEM concentration levels using different model approaches. Evaluation of particular processes governing Hg cycling in the atmosphere require more detailed analysis of its spatial and temporal variation.

Analysis of the inter-hemispheric gradient of GEM concentration is presented in Fig. 4. The figure shows the meridional distribution of both observed and model predicted concentration in the surface air. The later is split into two fractions contributed by anthropogenic and natural/secondary sources. As seen all four models reproduce the observed difference of GEM concentration between the Southern and Northern Hemispheres. The lowest concentrations (below $1\,\mathrm{ng/m^3}$) are typical for the high and temperate latitudes of the Southern Hemisphere. There is a weak maximum of zonal–mean GEM concentration (1.4-1.6 $\mathrm{ng/m3}$) in the temperate latitudes of the Northern Hemisphere corresponding to location of the majority of anthropogenic emission sources. The models predict some decrease of concentration further northward, which is not evident from the observations. It can be connected with overestimation of the oxidation chemistry in the Arctic or with underestimation of Hg re-emission from snow and seawater. As seen the inter-hemispheric gradient is largely formed by contribution of direct anthropogenic emissions which is larger in the Northern Hemisphere. Contribution of natural and secondary emissions also increases northward but the gradient is commonly smaller.

Statistics of the comparison of simulated and observed GEM concentration for different model experiments (see Table 2) is shown in Fig. 3 in terms of the spatial and temporal correlation coefficients and the relative bias. Details of the applied statistics is given in Section 2.5. In the BASE simulation all the models produce concentration distributions, which well agree with measurements (the spatial correlation coefficient is about 0.7 and the bias is around zero). On the other hand, the models differ in their ability to reproduce temporal variation of GEM in the surface air. The coefficient of temporal correlation between simulated and observed monthly mean values varies between -0.3 and 0.5. (Fig. 3(b)). Sprovieri et al. (2016a) found consistent seasonal cycle of GEM concentration observed at most measurement sites of both Northern and Southern Hemispheres with higher concentrations during winter and spring and lower concentrations in summer and fall. However, it should be noted that seasonal variation of monthly mean concentration is not significant at temperate and low latitudes where most of the sites are located and commonly does not exceed $\pm 20\%$. Therefore, reproduction of the GEM temporal variation is a challenging task for models taking into account absent data on seasonal variation of anthropogenic emissions used in the study (AMAP/UNEP, 2013b).

Switching off anthropogenic emissions (NoANT) leads to decrease of GEM levels in the atmosphere (the bias is -40%) and some decrease of spatial correlation with measurements. It is worth to say that spatial distribution of Hg concentration in this experiment is largely determined by model–specific natural and secondary emissions and, therefore, the change of spatial correlation considerably differs among the models. Removing anthropogenic emissions from the model simulations does not affect the temporal variation of the modelling result. In contrast, results of the experiment with no natural and secondary emissions (NoNAT) demonstrates significant improvement of temporal correlation with measurements for the models showed poor correlation in the BASE run. Besides, the exclusion of natural and secondary emissions leads to some decrease of spatial correlation and large negative bias (100%). Simulations with different chemical mechanisms (BrCHEM1, BrCHEM2, O3CHEM, OHCHEM) do not lead to considerable changes of both spatial distribution and temporal variation of GEM concentration in the surface air. Somewhat better spatial correlation was obtained for the oxidation reactions with Br (BrCHEM1) and OH radical (OHCHEM) and worse for the reaction with ozone (O3CHEM).

3.2 Reactive mercury

Oxidized Hg species composing RM originate in the atmosphere both from direct anthropogenic emissions and through oxidation of GEM in the gas phase, the aqueous phase of cloud water, and heterogeneously at various atmospheric interfaces (Ariya et al., 2015). Therefore, simulation of RM by contemporary models is much more challenging task taking into account incomplete current knowledge on Hg atmospheric chemistry as well as lack and uncertainty of measurement data (Gustin et al., 2015). Global distributions of RM concentration in the surface air simulated by the models for the BASE case is shown in Fig. 5. As seen the models predict considerably different spatial patterns of RM concentration. The concentration levels are comparable in industrial regions, which are affected by direct anthropogenic emissions, but differ significantly in remote regions where the influence of emissions weakens. Thus, the simulated patterns highly depend on applied chemical mechanisms and parameterisations of removal processes. Indeed, the models that apply ozone and/or OH oxidation chemistry in the BASE case (Figs. 5a, 5c, 5d) predict elevated RM concentrations at low latitudes (the tropics and the equatorial zone) due to high concentrations of these photo-oxidants (mainly, OH radical) in these regions (see Fig. S8 in the Supplement). On the other hand, application of the Br-derived chemistry (Fig. 5b) leads to the spatial pattern with elevated RM concentrations in the polar regions, particularly, of the Southern Hemisphere. It is in agreement with the spatial distribution of Br in the atmosphere (Fig. S6 in the Supplement). In addition, model parameterisation of dry deposition also considerably affects RM concentration in the surface air. Application of the effective RM removal in the marine boundary layer by sea-salt aerosol in GEOS-Chem (Holmes et al., 2010) results in lower RM concentrations over the oceans than those simulated by other models (Fig. 5b).

Scarce long-term observations of RM do not allow to reconstruct a reliable spatial trends on a global scale. Annual mean RM observations for the considered year are available only at 9 sites in North America, 2 sites in Europe, 1 site in the Arctic and 2 sites in the Southern Hemisphere (Fig. 1). Taking into account short lifetime of RM in the atmosphere with respect to deposition (Gustin et al., 2015; Ariya et al., 2015) this limited observations dataset can hardly characterize spatial variation of RM over the globe. Nevertheless, the measurements can be used for evaluation of the modelling results at particular locations. The models vary in their performance when reproducing measured values. The scatter plots of the model-to-measurement comparison in Fig. S3 in the Supplement demonstrate significantly poorer model agreement with observation than in the case of GEM. From 30% to 90% of the simulated values fall beyond the agreement range within a factor of 3. Besides, there is a general tendency to overestimate the observed concentrations. The level of overestimation varies among the sites and among the models and can be explained by a number of factors including uncertainties of the measurements associated with losses due to interference of oxidants and incomplete capture of GOM (Lyman et al., 2010; Huang and Gustin, 2015; Gustin et al., 2015), incorrect emissions speciation (Zhang et al., 2012; Amos et al., 2012; Kos et al., 2013; Bieser et al., 2014), and uncertainties of atmospheric chemistry (Weiss-Penzias et al., 2015; Ariya et al., 2015; Shah et al., 2016).

Figure 6 shows statistics of model-to-measurement comparison of RM air concentration for different model experiments. As it was mentioned above the models considerably overestimate observed values in the BASE case simulation. Similar over-

Atmos. Chem. Phys. Discuss., doi:10.5194/acp-2016-924, 2016
Manuscript under review for journal Atmos. Chem. Phys.
Published: 31 October 2016

estimation was observed by Kos et al. (2013) when simulating Hg oxidised forms in a series of model sensitivity runs. And it was attributed to significant extent to incorrect speciation of anthropogenic emissions with too high proportion of oxidized Hg forms. It is also confirmed by the NoANT experiment of the current study with zeroed out anthropogenic emissions that leads to the significantly lower positive or even negative bias (Fig. 6a). To reduce the effect of this uncertainty in the current study we use the modified speciation of emissions data for the model experiments focused on comparison of the chemical mechanisms with all Hg emissions treated as GEM (Section 2.4). The overprediction of observed RM concentrations by a factor of 2.5 was also found by Weiss-Penzias et al. (2015) for a number of high- and mid-elevation sites and it was connected with collection inefficiency of the KCl denuder used for GOM measurements (Gustin et al., 2013). The models differ in their ability to reproduce temporal variation of RM concentration (the correlation coefficient varies within the range -0.5–0.6 in the BASE case) (Fig. 6b). It is connected with both different chemical mechanisms applied in the standard model configurations (Table 1) and deviations in model treatment of removal processes responsible for dry and wet deposition. Exclusion of anthropogenic and natural/secondary emissions (NoANT and NoNAT) only slightly affect temporal correlation of the modelling results with observations. However, it should be pointed out once again that the emissions inventory used for the study ((AMAP/UNEP, 2013b)) does not resolve the intra-annual variability of anthropogenic emissions. So one can expect stronger effect of anthropogenic emissions on RM temporal variation. Among the chemical mechanisms the best correlation between modelled and observed values were obtained for reactions with Br (BrCHEM1 and BrCHEM2) followed by the OH oxidation mechanism (OHCHEM). Application of the reaction with O_3 leads to negative correlation with observations. Interesting to note that taken alone OH- and O_3-initiated chemistry predicts somewhat stronger oxidation of GEM in comparison with the Br chemistry that results in a positive bias of simulated RM concentrations (Fig. 6a).

More detailed analysis of the chemical oxidation mechanisms is presented in Fig. 7 in terms of comparison of simulated and observed RM/GEM ratios. Indeed, atmospheric RM originates either from direct emissions from anthropogenic sources or as a product of GEM oxidation in the atmosphere (Selin, 2009; Travnikov, 2012; Kos et al., 2013; Ariya et al., 2015). So in the immediate vicinity of emission sources the RM/GEM ratio reflects the speciation of Hg emissions, whereas in remote regions far away from any emissions it largely quantifies oxidative capability of the atmosphere. Given short life time of RM in the atmosphere with respect to deposition the influence of direct emissions on the RM/GEM ratio should quickly weaken with the distance from sources. Following the methodology suggested by Kos et al. (2013) we classified the sites used for the following analysis with respect to their remoteness from significant emission sources based on the model sensitivity run with the turned off Hg atmospheric chemistry. The simulated RM concentrations show (Fig. S5 in the Supplement) that all the selected sites (except one) can be classified as located far from sources (0-30 $\mathrm{pg\,m^{-3}}$). It agrees with characteristics of the North American sites given by Lan et al. (2012). The only site that is probably directly affected by anthropogenic emissions is Waldhof, Germany (Weigelt et al., 2013). Nevertheless, since both mean levels and seasonal variation of RM concentrations measured at this site does not differ significantly from others it was retained in the dataset. However, it should be noted that this analysis essentially depends upon the applied emissions data and can translate their uncertainties to the classification results.

Figure 7 shows comparison of simulated and observed annual mean RM/GEM ratios for different chemical mechanisms. Whiskers show standard deviation of monthly mean simulated and observed values. It should be pointer out that the observed

Atmos. Chem. Phys. Discuss., doi:10.5194/acp-2016-924, 2016
Manuscript under review for journal Atmos. Chem. Phys.
Published: 31 October 2016

values of RM/GEM (1-10 $\mathrm{pg\,ng^{-1}}$) correspond to background conditions of the continental boundary layer and are considerably lower those from mountain sites analysed by Weiss-Penzias et al. (2015) (10-100 $\mathrm{pg\,ng^{-1}}$). Exceptions are the site Alert, Canada located in the high Arctic (86 $\mathrm{pg\,ng^{-1}}$) and the elevated site Salt Lake City, USA (21 $\mathrm{pg\,ng^{-1}}$). It is interesting to note that the other elevated site Longobucco, Italy does not show similar increased RM/GEM values (9.5 $\mathrm{pg\,ng^{-1}}$). As seen from the figure the best qualitative agreement between the models and measurements is found in the experiment BrCHEM1 with the Br chemistry and one of the Br concentration datasets (Fig. 7a). Three of four models demonstrate good performance reproducing observations at most of the sites within a factor of 3. The fourth model (ECHMERIT) shows significant overestimation of the observed values, which is typical also for other model experiments (except for O3CHEM). Therefore, most probably it is not caused by the applied chemistry but by other factors such as removal processes. As it will be shown below the model tends to underestimate wet deposition of Hg that is mostly consists of scavenging of highly soluble RM. Application of the Br chemistry with the other Br concentration dataset (BrCHEM2) leads to less consistent results (Fig. 7b). Generally, the model-to-measurement deviations are within a factor of 5 except for the results of ECHMERIT discussed above. The RM/GEM ratios simulated by two other models vary from moderate underestimation to overestimation of the observed values. The inter-model difference can be caused both by discrepancies in formulation of removal processes and by particular implementation of the Br chemical mechanism (see Table 1). Somewhat similar results were obtained in the experiment with the OH chemistry (OHCHEM, Fig. 7d). The deviations between the modelled and measured RM/GEM are again mostly within a factor of 5 and the model-to-model difference is probably resulted from application of somewhat different reaction constants (Table 1). In contrast, application of the O_3-initiated chemistry leads to very consistent results (O3CHEM, Fig. 7c). The models predict some overestimation of the measured RM/GEM ratios with minimum scattering of the modelling results. On the other hand, the models tend to considerably underestimate intra-annual variation of monthly values shown by whiskers. None of the chemical mechanisms allows to reproduce high annual RM/GEM ratios (above 80 $\mathrm{pg\,ng^{-1}}$) observed at the Arctic site Alert, Canada (Fig. 7a-c). These high annual values are connected with intensive Hg oxidation during the springtime atmospheric mercury depletion events (AMDEs). Analysis of specific processes typical for the polar regions is beyond the scope of this paper. Discussion of results of the study focused on the polar regions can be found elsewhere (Angot et al., 2016).

More insight into the effect of different chemical mechanisms can be obtained from the analysis of RM/GEM seasonal variation. Figure 8 shows both measured and simulated variation of the monthly mean RM/GEM ratio averaged over selected sites. Since the seasonal variation of both RM and GEM differs in the Northern and Southern Hemispheres and majority of considered sites are located in North America and Europe we selected for this purpose only sites situated northward the Equator. Besides, we excluded the Arctic site (Alert) and two high elevated sites (Salt Lake City and Longobucco) to avoid effects of specific conditions of the polar regions and the free troposphere, respectively. Thus, the collection of sites characterises seasonality of Hg oxidation in the continental boundary layer of the northern temperate latitudes. As seen the observed values demonstrate a pronounced seasonal changes of RM/GEM with maximum in March and minimum in September (Fig. 8). Similar seasonal variation of Hg oxidised forms at background sites were observed in previous studies (Poissant et al., 2005; Sigler et al., 2009; Nair et al., 2012; Weigelt et al., 2013). The chemical oxidation mechanisms differ in their ability to reproduce the observed seasonal variation. Application of the Br chemistry with both Br concentration datasets (BrCHEM1 and BrCHEM2)

Atmos. Chem. Phys. Discuss., doi:10.5194/acp-2016-924, 2016
Manuscript under review for journal Atmos. Chem. Phys.
Published: 31 October 2016

provides the best agreement with measurements reproducing the maximum RM/GEM ratios during spring months by three of four models (Figs. 8a and 8b). The fourth model predicts the highest ratios during late summer independently of applied chemical mechanism that is probably determined by other factors including meteorological conditions and removal processes. The simulated maximum of RM/GEM in the spring months can be explained by high Br concentrations in both the free troposphere and the boundary layer of the Northern Hemisphere (Fig. S9 in the Supplement). Model simulations with OH chemistry (OHCHEM) predict the maximum RM/GEM ratios during summer months (Fig. 8d) in accordance with seasonal variation of OH concentration which is also the highest in summer (Fig. S11 in the Supplement). Use of the O_3-initiated chemistry does not lead to any significant variation of Hg oxidation during the year (Fig. 8c).

3.3 Wet deposition

Wet deposition is one of the major removal mechanisms responsible for exchange of Hg between the atmosphere and the Earth surface (Travnikov, 2012; Swartzendruber and Jaffe, 2012). It is largely determined by precipitation events, on one hand, and by availability of soluble Hg forms in the atmosphere, on the other. Given poor solubility of GEM (Clever et al., 1985; Ariya et al., 2015) Hg wet deposition mostly consists of scavenging of Hg oxidized forms (GOM and PBM). Therefore, Hg concentration in precipitation and, ultimately, wet deposition flux largely depends upon three factors – direct emissions of oxidized Hg from anthropogenic sources, Hg oxidation in the atmosphere, and precipitation amount. Figure 9 shows spatial patterns of annual mean Hg wet deposition simulated by the four models according to the BASE case. Available measurements are also shown in the same colour palette. Generally, the simulated deposition maps have similar spatial distributions reflecting the influence of the global precipitation pattern and major emission regions. High deposition fluxes are characteristics of Asia, Europe and North America where significant anthropogenic sources are located as well as of regions with intensive precipitation (e.g. the Inter-tropical Convergence Zone). The lowest wet deposition fluxes are in dry regions (e.g. in Northern Africa, Greenland, and Antarctica). Divergences among the modelling results are mostly explained by different chemical mechanisms applied by the models in the BASE case. For instance, GEOS-Chem predicts elevated wet deposition in the high latitudes of the Southern Hemisphere where high Br concentrations (Fig. S6 in the Supplement) excite intensive oxidation of GEM in the atmosphere (Fig. 9b). On the other hand, significant deposition fluxes are simulated in the high Arctic by GEM-MACH-Hg (Fig. 9c) due to application of parameterisations of physical and chemical processes occurring during AMDEs. The models relatively well agree with available long-term observations of Hg wet deposition. The model-to-measurement deviations commonly do not exceed a factor of two (Fig. S4 in the Supplement). However, it should be noticed that available observations of Hg wet deposition are still mostly restricted by two regions – North America and Europe. Only few measurements are available in other regions and, in particular, in the Southern Hemisphere.

Statistics of the comparison of simulated and observed wet deposition fluxes is given in Fig. 10. Results of the BASE case simulation are characterized by significant temporal correlation with with measurements (0.4-0.6) and some slight bias ($\pm 40\%$) which is variable among the models. Direct anthropogenic emissions of oxidized Hg considerably contributes to wet deposition and so its elimination (NoANT) results in noticeable deposition decrease characterized by negative bias. In contrast to anthropogenic emissions natural/secondary sources emit Hg mostly as GEM. Nevertheless, turning off natural/secondary

Atmos. Chem. Phys. Discuss., doi:10.5194/acp-2016-924, 2016
Manuscript under review for journal Atmos. Chem. Phys.
Published: 31 October 2016

emissions (NoNAT) also leads to substantial decrease of wet deposition indicating their indirect effect through GEM oxidation to the soluble Hg forms with subsequent scavenging by precipitation. Temporal correlation of wet deposition is not sensitive to emission changes. That is not wondering because the anthropogenic emissions inventory used in the study does not contains information on temporal variation of emissions. The oxidation chemistry considerably affects both general level and temporal variation of Hg wet deposition. The Br oxidation mechanism provides relatively good correlation with observations but there is a large difference between results for two different Br concentration datasets (BrCHEM1 and BrCHEM2) in terms of relative bias. The highest correlation is obtained for the OH oxidation chemistry (OHCHEM). It should be noticed that differently from other models used for this study, ECHMERIT is based on the ECHAM climate model that is expected to reproduce the actual weather behaviour, in particular precipitations events, over a relatively longer temporal period and wider areas, and may diverge on shorter time scales and smaller regional areas (see for example Angálil et al. (2016)). Since simulated Hg wet deposition is largely driven by the model generated precipitation we prefer to not include the results of the climate-based ECHMERIT model in the following analysis to avoid biasing the statistics.

Similar to RM concentration wet deposition of Hg is a parameter that is strongly determined by atmospheric oxidation chemistry (Selin and Jacob, 2008; Kos et al., 2013). Therefore, analysis of wet deposition can be also applied for evaluation of chemical mechanisms of Hg oxidation in the atmosphere. Unlike RM concentration levels measured at ground-based sites near the surface wet deposition measurements characterize processes occurring in the free troposphere since the scavenging of soluble Hg takes place both in the cloud environment and along the whole path of convective or large-scale precipitation. Comparison of simulated and observed wet deposition fluxes for different model experiments is shown in Fig. 11. Both measured and simulated values are averaged over different groups of sites including 7 groups in North America following the latitudinal ranges suggested by Selin and Jacob (2008), 3 groups in Europe (Southern Europe, Western Europe and Northern Europe), and 1 group per region in Asia, Australia, and the Indian Ocean (see Table S3 in the Supplement). As seen from the figure simulations with the Br oxidation mechanism and the first set of Br concentration data (BrCHEM1) satisfactorily reproduces observations (Fig. 11a). The models relatively well agree with each other and the mode-to-measurement deviations mostly do not exceed a factor of 2. However, all the models overpredict low deposition fluxes (below $10\,\mathrm{ng\,m^{-2}\,day^{-1}}$) measured in Asia and in the Southern Hemisphere. The overestimation of Hg wet deposition at two high altitude Asian sites (Mt. Waliguan and Mt. Ailao) can be connected with inability of the global models with rough spatial resolution to reproduce complex meteorological conditions of the mountain regions. The overprediction at the southern sites (Cape Grim and Amsterdam Island) might be explained by very high Br concentrations predicted by the first dataset at temperate latitudes of the Southern Hemisphere (Fig. S6 in the Supplement). Application of the same mechanism with the other Br dataset leads to considerably lower levels of wet deposition (Fig. 11b) due to use of much smaller Br concentrations, particularly, in the free troposphere (Fig. S6 in the Supplement). Thus, uncertainties of available estimates of Br atmospheric concentration largely affect simulation results of the Hg cycling in the atmosphere. Model simulations with the O_3 and OH oxidation mechanisms (O3CHEM and OHCHEM) also provide reasonable agreement between the modelling results and measurements (Figs. 11c and 11d). In both cases the simulated values well correlate with the observed ones and deviations are mostly within a factor of 2. The OH oxidation chemistry

Atmos. Chem. Phys. Discuss., doi:10.5194/acp-2016-924, 2016
Manuscript under review for journal Atmos. Chem. Phys.
Published: 31 October 2016

Atmospheric Chemistry and Physics
Open Access
Discussions

provides somewhat better agreement in terms of the slope of regression line that is closer to the reference 1:1 line indicating better reproduction of both low and high wet deposition fluxes.

More information on the performance of different chemical mechanisms can be obtained from the analysis of seasonal patterns of wet deposition. Since the majority of available wet deposition measurements are at sites located in North America and Europe we focus our further discussion on these two regions. Figure 12 shows comparison of modelled and measured temporal variation of monthly mean wet deposition flux averaged over sites located in North America and Europe. The monthly fluxes were normalized by the annual average value to remove absolute differences among the models and reveal peculiarities of seasonal changes. As seen the observations demonstrate well pronounced seasonal cycle with maximum in summer and minimum during the cold season (winter and early spring). Similar seasonal variations has been reported in previous studies (Guentzel et al., 2001; Keeler et al., 2005; Choi et al., 2008; Prestbo and Gay, 2009; Sprovieri et al., 2016b). Sprovieri et al. (2016b) attributes these seasonal changes to variation of meteorological conditions (mostly, precipitation amount), more effective Hg scavenging by rain compared to snow and changes in availability of soluble Hg. As seen from Figs. 12i and 12j precipitation amount measured in North America and Europe, respectively, does not reveal similar seasonality to explain intra-annual variation of wet deposition. Seasonal variation of precipitation amount in North America demonstrate similar pattern with maximum in summer and minimum in winter but the amplitude of the variation is much smaller than that of wet deposition. Average precipitation amount in Europe does not have evident seasonal pattern. Availability of soluble Hg in the free troposphere highly depends on the oxidation chemistry. Therefore, different chemical mechanisms should differently affect seasonality of wet deposition. Indeed, both model runs with the Br oxidation chemistry (BrCHEM1 and BrCHEM2) predict maximum in wet deposition during the spring months instead of summer (Figs. 12a-d) following the seasonal variation of Br concentration in the atmosphere (Fig. S9 in the Supplement). Simulations with the O_3-initiated chemistry (O3CHEM) provide much lower seasonality of deposition flux (Figs. 12e-f). In contrast, application of the OH chemistry (OHCHEM) well reproduces the observed seasonal variation of wet deposition in both considered regions (Figs. 12g-h). Similar results were obtained by other researches. Selin and Jacob (2008) simulated Hg wet deposition over the United States applying the combined OH/O_3 oxidation chemistry and successfully reproduced the measured seasonal variation. They attributed the summer maximum in the Northeast to GEM photochemical oxidation and to inefficient scavenging by snow in winter. Holmes et al. (2010) compared the Br mechanism vs. the OH/O_3 mechanism simulating the Hg global cycle. They found that the OH/O_3 chemistry allows better simulating the southeast summer maximum in Hg wet deposition, where it reflects scavenging of GOM from the free troposphere by deep convection. Kos et al. (2013) also performed a number of sensitivity runs with different parameterizations of chemical processes and showed that using the OH oxidation chemistry improves simulations of the seasonal cycle of wet deposition in North America. Taking into account that Hg wet deposition is largely defined by oxidation of GEM (Selin and Jacob, 2008), we can expect significant effect of the OH-initiated chemistry on Hg oxidation in the free troposphere. On the other hand, when comparing this conclusion with the results presented in Section 3.2, where it was shown that seasonal dynamics of the RM/GEM ratio observed at ground-based sites is dominated by the Br oxidation chemistry, one can assume possibility of different Hg oxidation mechanisms occurring concurrently in different parts of the atmosphere.

Atmos. Chem. Phys. Discuss., doi:10.5194/acp-2016-924, 2016
Manuscript under review for journal Atmos. Chem. Phys.
Published: 31 October 2016

4 Conclusions

The presented study provides a complex analysis of processes governing Hg cycling in the atmosphere involving both measurement data from ground-based sites and application of chemical transport models. A variety of long-term measurements of GEM and RM concentration as well as wet deposition flux has been compiled from different global and regional monitoring networks. Four contemporary global-scale transport models for Hg were applied both in their state-of-the-art configurations and for a number of numerical experiments aimed at evaluation of particular processes. Results of the model simulation were evaluated against measurements. The models predict similar global spatial patterns of GEM concentration in the near-surface air in spite of significant deviations in applied parameterizations of physical and chemical processes. The model-measurement divergence does not commonly exceed $\pm 30\%$. All four models reproduce the observed decrease of GEM concentration between the Northern and Southern Hemispheres. As it follows from the analysis the inter-hemispheric gradient is largely formed by the spatial distribution of anthropogenic emissions which prevail in the Northern Hemisphere. Contribution of natural and secondary emissions enhances the south-to-north gradient but their effect is less significant. The oxidation chemistry does not affect considerably both spatial distribution and temporal variation of GEM concentration in the surface air.

Model simulation of RM is much more challenging task taking into account incomplete current knowledge on Hg atmospheric chemistry as well as lack and uncertainty of measurement data. The models differ considerably in prediction of spatial and temporal patterns of RM concentration. The simulated RM levels are comparable in industrial regions, which are affected by direct anthropogenic emissions, but differ significantly in remote regions where the influence of emissions weakens. Thus, the simulated patterns highly depend on applied chemical mechanisms and parameterisations of removal processes. The model-to-measurement comparison demonstrate significantly poorer model agreement with observations than in the case of GEM. From 30% to 90% of the simulated values fall beyond the agreement range within a factor of 3. Besides, there is a general tendency to overestimate the observed RM concentrations, which can be attributed to incorrect speciation of Hg emissions, uncertainties of Hg atmospheric chemistry, and incomplete RM capture by measurements. Atmospheric chemistry largely affects the RM/GEM ratio in the atmosphere. Application of the Br chemistry provides the best agreement with observations reproducing both general levels and seasonal variation of the RM/GEM ratio in the near-surface layer. However, global distribution of Br concentration is highly uncertain. Model simulations with the OH chemical mechanism predict shifting the maximum RM/GEM ratios from spring to summer, whereas the $\mathrm{O_3}$-initiated chemistry does not lead to significant seasonal variation of Hg oxidation.

Wet deposition maps simulated by different models have similar spatial distributions reflecting the influence of the global precipitation pattern and situation of major emission regions. High deposition fluxes are characteristics of Asia, Europe and North America where significant anthropogenic sources are located as well as of regions with intensive precipitation. The models relatively well agree with available long-term observations of Hg wet deposition. The model-to-measurement deviations commonly do not exceed a factor of 2. However, there is a tendency to overpredict low deposition fluxes measured in Asia and in the Southern Hemisphere. Similar to RM concentrations wet deposition of Hg in background regions is strongly determined by the atmospheric oxidation chemistry. Model runs with the Br oxidation mechanism predict maximum in wet deposition in spring instead of summer as observed at monitoring sites located in North America and Europe. The O_3 chemistry does not provide significant seasonal changes of wet deposition flux in these regions. Application of the OH chemistry allows reproducing both the periods of maximum and minimum values and the amplitude of observed seasonal variation.

Thus, performance of the considered Hg oxidation mechanisms differs in reproduction of different observed parameters that can imply possibility of more complex chemistry and multiple pathways of Hg oxidation occurring concurrently in various parts of the atmosphere. More extensive measurements of both RM including identification of Hg chemical species and wet deposition are needed in various geographical regions and under different climatic conditions for further improvement of Hg chemical transport models.

Author contributions. The names after the first author in the above list are in alphabetical order and all authors have made significant contribution. In particular,
Measurements: H. Angot, P. Artaxo, M. Bencardino, F. D'Amore, M. C. Diéguez, A. Dommergue, R. Ebinghaus, X. B. Feng, O. Magand, L. Martin, N. Mashyanov, N. Pirrone, R. Ramachandran, K. A. Read, F. Sena, F. Sprovieri, D. Wip, I. Wängberg;
Modelling: J. Bieser, A. Dastoor, F. De Simone, C. N. Gencarelli, I. M. Hedgecock, V. Matthias, A. Ryjkov, N. E. Selin, S. Song, O. Travnikov, X. Yang.

Acknowledgements. The authors wish to thank David Gay from the National Atmospheric Deposition Program (NADP) and the principal investigators for the AMNet sites (E. Edgerton, W. Luke, J. Chaffin, R. Callison, B. Call, M. Pendleton, E. Miller, and M. Allen) for providing the Hg measurement data used in this study. The authors also gratefully acknowledge the Canadian Air and Precipitation Monitoring Network (CAPMoN) for the data and the National Atmospheric Chemistry (NAtChem) Database and Analysis Facility of Environment Canada (www.ec.gc.ca/natchem) for Internet provision of the data. This study was financially supported in part by the EU FP7-ENV-2010 project "Global Mercury Observation System" (GMOS, Grant Agreement n° 265113). Noelle E. Selin and Shaojie Song also acknowledge the U.S. National Science Foundation Atmospheric Chemistry Program (Grant # 1053648) for the financial support.

References

AMAP/UNEP, Technical Background Report for the Global Mercury Assessment 2013a. Arctic Monitoring and Assessment Programme, Oslo, Norway / UNEP Chemicals Branch, Geneva, Switzerland. vi + 263 pp., 2013, available at http://www.unep.org/chemicalsandwaste/Mercury/ReportsandPublications/tabid/3593/Default.aspx, access: 1 August 2016.

AMAP/UNEP, Geospatially distributed mercury emissions dataset 2010v1, 2013b, http://www.amap.no/mercury-emissions, access: 1 August 2016.

AMAP/UNEP, Global Mercury Modelling: Update of Modelling Results in the Global Mercury Assessment 2013. Arctic Monitoring and Assessment Programme, Oslo, Norway/UNEP Chemicals Branch, Geneva, Switzerland. iv + 32 pp., 2015, available at http://www.unep.org/chemicalsandwaste/Mercury/ReportsandPublications/tabid/3593/Default.aspx, access: 1 August 2016.

AMNet: Atmospheric Mercury Network. http://nadp.sws.uiuc.edu/amn/, access: 1 August 2016.

Amos, H. M., Jacob, D. J., Holmes, C. D., Fisher, J. A., Wang, Q., Yantosca, R. M., Corbitt, E. S., Galarneau, E., Rutter, A. P., Gustin, M. S., Steffen, A., Schauer, J. J., Graydon, J. A., St Louis, V. L., Talbot, R. W., Edgerton, E. S., Zhang, Y., and Sunderland, E. M.: Gas-particle partitioning of atmospheric Hg(II) and its effect on global mercury deposition, Atmos. Chem. Phys., 12, 591-603, doi:10.5194/acp-12-591-2012, 2012.

Angálil, O., Perkins-Kirkpatrick, S., Alexander, L. V., Stone, D., Donat, M. G., Wehner, M., Shiogama, H., Ciavarella, A., Christidis, N.: Comparing regional precipitation and temperature extremes in climate model and reanalysis products, Weather and Climate Extremes, 13, 35-43, doi:10.1016/j.wace.2016.07.001, 2016.

Angot, H., Dastoor, A., De Simone, F., Gårdfeldt, K., Gencarelli, C. N., Hedgecock, I. M., Langer, S., Magand, O., Mastromonaco, M. N., Nordstrøm, C., Pfaffhuber, K. A., Pirrone, N., Ryjkov, A., Selin, N. E., Skov, H., Song, S., Sprovieri, F., Steffen, A., Toyota, K., Travnikov, O., Yang, X., and Dommergue, A.: Chemical cycling and deposition of atmospheric mercury in polar regions: review of recent measurements and comparison with models, Atmos. Chem. Phys., 16, 10735-10763, doi:10.5194/acp-16-10735-2016, 2016.

Ariya, P. A., Amyot, M., Dastoor, A., Deeds, D., Feinberg, A., Kos, G., Poulain, A., Ryjkov, A., Semeniuk, K., Subir, M., and Toyota, K.: Mercury Physicochemical and Biogeochemical Transformation in the Atmosphere and at Atmospheric Interfaces: A Review and Future Directions, Chem. Rev., 15 (10), 3760?3802, doi: 10.1021/cr500667e, 2015.

Baker, K. R. and Bash, J. O.: Regional Scale Photochemical Model Evaluation of Total Mercury Wet Deposition and Speciated Ambient Mercury. Atmos. Environ., 49, 151-162, 2012.

Balabanov, N., Shepler, B., Peterson, K.: Accurate global potential energy surface and reaction dynamics for the ground state of $HgBr_2$. J. Phys. Chem. A, 109, 8765-8773, 2005.

Bey, I., Jacob, D. J., Yantosca, R. M., Logan, J. A., Field, B. D., Fiore, A. M., Li, Q., Liu, H. Y., Mickley, L. J., and Schultz, M. G.: Global modeling of tropospheric chemistry with assimilated meteorology: Model description and evaluation, J. Geophys. Res.-Atmos., 106, 23073?23095, doi:10.1029/2001jd000807, 2001.

Bieser, J., De Simone, F., Gencarelli, C., Geyer, B., Hedgecock, I., Matthias, V., Travnikov, O., and Weigelt, A.: A diagnostic evaluation of modeled mercury wet depositions in Europe using atmospheric speciated high-resolution observations, Environ. Sci. Pollut. Res., 21, 9995–10012, doi:10.1007/s11356-014-2863-2, 2014.

Calvert, J. G. and Lindberg, S. E.: Mechanisms of mercury removal by O3 and OH in the atmosphere, Atmos. Environ., 39, 3355-3367, oi:10.1016/j.atmosenv.2005.01.055, 2005.

Cohen, M.D., Draxler, R.R., Artz, R.S., Gustin, M., Han, Y-J., Holsen, T.M., Jaffe, D., Kelley, P., Lei, H., Loughner, C., Luke, W., Lyman, S., Niemi, D. Pacyna, J.M., Pilote, M., Poissant, L., Ratte, D., Ren, X., Steenhouisen, F., Tordon, R., and Wilson, S.: Modeling the global atmospheric transport and deposition of mercury to the Great Lakes. Elementa: Science of the Anthropocene, 4, 000118, doi: 10.12952journal.elementa.999118, 2016.

Choi, H.-D., Sharac, T. J., and Holsen, T. M.: Mercury deposition in the Adirondacks: A comparison between precipitation and throughfall, Atmospheric Environment, 42, 1818-1827, 2008.

Christensen, J., Brandt, J., Frohn, L., Skov, H.: Modelling of Mercury in the Arctic with the Danish Eulerian Hemispheric Model. Atmos. Chem. Phys., 4, 2251-2257, 2004.

Clever, H. L., Johnson, S. A., Derrick, M. E.: The solubility of mercury and some sparingly soluble mercury salts in water and aqueous electrolyte solutions. J. Phys. Chem. Ref. Data, 14, 631-680, 1985.

Cole, A. S., Steffen, A., Pfaffhuber, K. A., Berg, T., Pilote, M., Poissant, L., Tordon, R., and Hung, H.: Ten-year trends of atmospheric mercury in the high Arctic compared to Canadian sub-Arctic and mid-latitude sites, Atmos. Chem. Phys., 13, 1535-1545, doi:10.5194/acp-13-1535-2013, 2013.

Cremer, D., Kraka, E., and Filatov, M.: Bonding in Mercury Molecules Described by the Normalized Elimination of the Small Component and Coupled Cluster Theory, Chem. Phys. Chem., 9, 2510-2521, doi:10.1002/cphc.200800510, 2008.

Dastoor, A. P., and Larocque, Y.: Global circulation of atmospheric mercury: a modelling study, Atmospheric Environment, 38, 147-161, 2004.

Dastoor, A. P., Davignon, D., Theys, N., Van Roozendael, M., Steffen, A., and Ariya, P. A.: Modeling dynamic exchange of gaseous elemental mercury at polar sunrise, Environmental Science and Technology, 42, 5183-5188, 2008.

Dastoor, A., Ryzhkov, A., Durnford, D., Lehnherr, I., Steffen, A., and Morrison, H.: Atmospheric mercury in the Canadian Arctic. Part II: Insight from modeling, Sci. Total Environ., 509-510, 16-27, doi: 10.1016/j.scitotenv.2014.10.112, 2015.

De Simone, F., Gencarelli, C. N., Hedgecock, I. M., and Pirrone, N.: Global atmospheric cycle of mercury: a model study on the impact of oxidation mechanisms, Environ. Sci. Ppollut. R., 21, 4110-4123, 2014.

De Simone, F., Cinnirella, S., Gencarelli, C. N., Yang, X., Hedgecock, I. M., and Pirrone, N.: Model study of global mercury deposition from biomass burning, Environ. Sci. Technol., 49, 6712-6721, 2015.

De Simone, F., Cinnirella, S., Gencarelli, C. N., Carbone, F., Hedgecock, I. M., and Pirrone, N.: Particulate-Phase Mercury Emissions during Biomass Burning and Impact on Resulting Deposition: a Modelling Assessment, Atmos. Chem. Phys. Discuss., doi:10.5194/acp-2016-685, in review, 2016.

Dibble, T. S., Zelie, M. J., and Mao, H.: Thermodynamics of reactions of ClHg and BrHg radicals with atmospherically abundant free radicals, Atmos. Chem. Phys., 12, 10271-10279, 2012.

Donohoue, D. L., Bauer, D., Cossairt, B., and Hynes, A. J.: Temperature and Pressure Dependent Rate Coefficients for the Reaction of Hg with Br and the Reaction of Br with Br: A Pulsed Laser Photolysis-Pulsed Laser Induced Fluorescence Study, J. Phys. Chem. A, 110, 6623-6632, doi: 10.1021/jp054688j, 2006.

Durnford, D., Dastoor, A., Figueras-Nieto, D., and Ryjkov, A.: Long range transport of mercury to the Arctic and across Canada, Atmospheric Chemistry and Physics, 10, 6063-6086, 2010.

Durnford, D., Dastoor, A., Ryzhkov, A., Poissant, L., Pilote, M., and Figueras-Nieto, D.: How relevant is the deposition of mercury onto snowpacks? – Part 2: A modeling study, Atmos. Chem. Phys., 12, 9251-9274, 10.5194/acp-12-9251-2012, 2012.

ECMWF: European Centre for Medium-Range Weather Forecasts, http://www.ecmwf.int/en/forecasts/dataset, access: 1 August 2016.

EMEP: The European Monitoring and Evaluation Programme, EBAS database, http://ebas.nilu.no/Default.aspx, access: 1 August 2016.

Emmons, L. K., Walters, S., Hess, P. G., Lamarque, J. F., Pfister, G. G., Fillmore, D., Granier, C., Guenther, A., Kinnison, D., Laepple, T., Orlando, J., Tie, X., Tyndall, G., Wiedinmyer, C., Baughcum, S. L., and Kloster, S.: Description and evaluation of the Model for Ozone and Related chemical Tracers, version 4 (MOZART-4), Geosci. Model Dev., 3, 43-67, 10.5194/gmd-3-43-2010, 2010.

Fitzgerald, W. F., Engstrom, D. R., Mason, R. P., Nater, E. A.: The case for atmospheric mercury contamination in remote areas, Environ. Sci. Technol, 32, 1-7, 1998.

Gay, D., Schmeltz, D., Prestbo, E., Olson, M., Sharac, T., and Tordon, R.: The atmospheric mercury network: measurement and initial examination of an ongoing atmospheric mercury record across North America, Atmospheric Chemistry and Physics, 13, 10 521?10 546, 2013.

Gbor, P. K., Wen, D., Meng, F., Yang, F., Sloan, J. J.: Sloan Modeling of mercury emission, transport and deposition in North America. Atmos. Environ., 41, 1135-49, 2007.

Gencarelli, C. N., De Simone, F., Hedgecock, I. M., Sprovieri, F., Pirrone, N.: Development and Application of a Regional-Scale Atmospheric Mercury Model Based on WRF/Chem: A Mediterranean Area Investigation. Environ. Sci. Pollut. Res., 21, 4095-4109. 2014.

GMOS: Global Mercury Observation System, Spatial Data Infrastructure, http://www.gmos.eu/sdi/, access: 1 August 2016.

Goodsite, M. E., Plane, J. M. C., and Skov, H. A Theoretical Study of the Oxidation of Hg0 to HgBr2 in the Troposphere. Environ. Sci. Technol., 38, 1772-1776, 2004.

Goodsite, M. E., Plane, J. M. C., and Skov, H.: Correction to A Theoretical Study of the Oxidation of Hg^0 to $HgBr_2$ in the Troposphere, Environ. Sci. Technol., 46, 5262, 2012.

Granier, C., Lamarque, J., Mieville, A., Muller, J., Olivier, J., Orlando, J., Peters, J., Petron, G., Tyndall, G., Wallens, S.: POET, a database of surface emissions of ozone precursors, available at http://www.aero.jussieu.fr/projet/ACCENT/POET.php, 2005, access: 1 August 2016.

Gratz, L. E., Ambrose, J. L., Jaffe, D. A., Shah, V., Jaeglé, L., Stutz, J., Festa, J., Spolaor, M., Tsai, C., Selin, N. E., Song, S., Zhou, X., Weinheimer, A. J., Knapp, D. J., Montzka, D. D., Flocke, F. M., Campos, T. L., Apel, E., Hornbrook, R., Blake, N. J., Hall, S., Tyndall, G. S., Reeves, M., Stechman, D., Stell, M.: Oxidation of mercury by bromine in the subtropical Pacific free troposphere, Geophys. Res. Lett. 42(23), 10,494-10,502, 2015.

Guentzel, J. L., Landing, W. M., Gill, G. A., and Pollman, C. D.: Processes Influencing Rainfall Deposition of Mercury in Florida, Environ. Sci. Technol., 35, 863-873, 2001.

Gustin, M. S.: Exchange of Mercury between the Atmosphere and Terrestrial Ecosystems, in: Liu, G., Cai, Y. and N. O'Driscoll (Eds.), Environmental Chemistry and Toxicology of Mercury, John Wiley & Sons, Inc., Hoboken, NJ, USA, 423-451, doi: 10.1002/9781118146644.ch13, 2012.

Gustin, M. S., Weiss-Penzias, P. S., and Peterson, C.: Investigating sources of gaseous oxidized mercury in dry deposition at three sites across Florida, USA, Atmos. Chem. Phys., 12, 9201-9219, doi:10.5194/acp-12-9201-2012, 2012.

Gustin, M. S., Huang, J., Miller, M. B., Finley, B. D., Call, K., Ambrose, J. L., Peterson, C., Lyman, S. N., Everhart, S., Bauer, D., Remeika, J., Hynes, A., Jaffe, D. A., and Lindberg, S. E.: RAMIX - a step towards understanding mercury atmospheric chemistry and Tekran® observations, Environ. Sci. Technol., 47, 7295-7306, 2013.

Gustin, M. S., Amos, H. M., Huang, J., Miller, M. B., and Heidecorn K.: Measuring and modeling mercury in the atmosphere: a critical review, Atmos. Chem. Phys., 15, 5697-5713, doi:10.5194/acp-15-5697-2015, 2015.

Hall, B.: The gas phase oxidation of mercury by ozone. Water Air Soil Poll., 80, 301-315, 1995.

Hedgecock, I. M. and Pirrone, N.: Chasing quicksilver: Modeling the atmospheric lifetime of Hg-(g)(0) in the marine boundary layer at various latitudes, Environmental Science and Technology, 38, 69-76, 2004.

Holmes, C. D., Jacob D. J., Mason R. P., Jaffe D. A.: Sources and deposition of reactive gaseous mercury in the marine atmosphere, Atmospheric Environment 43(14), 2278-2285, 2009.

Holmes, C. D., Jacob, D. J., Corbitt, E. S., Mao, J., Yang, X., Talbot, R., and Slemr, F.: Global atmospheric model for mercury including oxidation by bromine atoms, Atmos. Chem. Phys., 10, 12037-12057, 2010.

Huang, J. and Gustin, M. S.: Impacts of relative humidity on GOM measurements, Environ. Sci. Technol., 49, 6102?6108, doi:10.1021/acs.est.5b00098, 2015.

Hynes, A. J., Donohoue, D. L., Goodsite, M. E., and Hedgecock, I. M.: Our current understanding of major chemical and physical processes affecting mercury dynamics in the atmosphere and at the air-water/terrestrial interfaces, in: Mercury Fate and Transport in the Global Atmosphere, edited by: Mason, R. and Pirrone, N., Springer, New York, 427-457, 2009.

Jung, G., Hedgecock, I. M., and Pirrone, N.: ECHMERIT V1.0 - a new global fully coupled mercury-chemistry and transport model, Geosci. Model Dev., 2, 175-195, 10.5194/gmd-2-175-2009, 2009.

Keeler, G., Gratz, L., and Al-wali, K.: Long-term Atmospheric Mercury Wet Deposition at Underhill, Vermont, Ecotoxicology, 14, 71-83, 2005.

Kos, G., Ryzhkov, A., Dastoor, A., Narayan, J., Steffen, A., Ariya, P. A., and Zhang, L.: Evaluation of discrepancy between measured and modelled oxidized mercury species, Atmos. Chem. Phys., 13, 4839-4863, 2013.

Krabbenhoft, D. P. and Sunderland, E. M.: Global change and mercury. Science, 341, 1457-1458, 2013.

Lan, X., Talbot, R., Castro, M., Perry, K., and Luke, W.: Seasonal and diurnal variations of atmospheric mercury across the US determined from AMNet monitoring data, Atmos. Chem. Phys., 12, 10569-10582, doi:10.5194/acp-12-10569-2012, 2012.

Lin, C.-J., Pongprueksa, P., Lindberg, S. E., Pehkonen, S. O., Byun, D. and Jang, C.: Scientific uncertainties in atmospheric mercury models I: Model science evaluation. Atmospheric Environment 40, 2911-2928, 2006.

Lindberg, S. E. and Stratton, W. J.: Atmospheric mercury speciation: concentrations and behavior of reactive gaseous mercury in ambient air, Environ. Sci. Technol., 32, 49-57, 1998.

Lohman, K., Seigneur, C., Gustin, M., Lindberg, S.: Sensitivity of the global atmospheric cycle of mercury to emissions, Applied Geochemistry, 23, 454-466, 2008.

Lyman, S. N., Jaffe, D. A., and Gustin, M. S.: Release of mercury halides from KCl denuders in the presence of ozone, Atmos. Chem. Phys., 10, 8197?8204, doi:10.5194/acp-10-8197-2010, 2010.

Lyman, S. N. and Jaffe, D. A.: Formation and fate of oxidized mercury in the upper troposphere and lower stratosphere, Nat. Geosci., 5, 114-117, 2011.Jaeglé

Mahaffey, K.R., Clickner, R. P., and Bodurow, C. C.: Blood organic mercury and dietary mercury intake: National Health and Nutrition Examination Survey, 1999 and 2000, Environmental Health Perspectives, 112(5), 562-670, 2004.

Mason, R. P. and Sheu, G.R.: Role of the ocean in the global mercury cycle, Global Biogeochem. Cycles, 16(4), 1093, doi:10.1029/2001GB001440, 2002.

Mason, R.: Mercury emissions from natural processes and their importance in the global mercury cycle, in: Mercury fate and transport in the global atmosphere, in: Pirrone, N. and Mason, R. P. (Eds.): Mercury Fate and Transport in the Global Atmosphere: Emissions, Measurements, and Models, Springer, pp. 173-191, 2009.

Mason, R. P., Choi, A. L., Fitzgerald, W. F., Hammerschmidt, C. R., Lamborg, C. H., Soerensen, A. L., Sunderland, E. M.: Mercury biogeochemical cycling in the ocean and policy implications, Environmental Research, 119, 101-117, 2012.

Munthe, J.: The aqueous oxidation of elemental mercury by ozone, Atmos. Environ., 26, 1461-1468, 1992.

Nair, U. S., Wu, Y., Walters, J., Jansen, J., Edgerton, E. S.: Diurnal and seasonal variation of mercury species at coastal suburban, urban, and rural sites in the southeastern United States. Atmos. Environ. 47, 499-508, 2012.

NADP/MDN: National Atmospheric Deposition Program (NRSP-3), Mercury Deposition Network (MDN), NADP Program Office, Illinois State Water Survey, 2204 Griffith Dr., Champaign, IL 61820, http://nadp.sws.uiuc.edu/MDN/, access: 1 August 2016.

NAtChem: The Canadian National Atmospheric Chemistry Database And Analysis System. http://www.ec.gc.ca/natchem/, access: 1 August 2016.

Obrist, D., Tas, E., Peleg, M., Matveev, V., Faïn, X., Asaf, D., Luria, M.: Bromine-induced oxidation of mercury in the mid-latitude atmosphere. Nature Geoscience 4, 22-26, 2011.

Pan, L., Lin, C.-J., Carmichael, G. R., Streets, D. G., Tang, Y., Woo, J.-H., Shetty, S. K., Chu, H.-W., Ho, T. C., Friedli, H. R.: Study of Atmospheric Mercury Budget in East Asia Using STEM-Hg Modeling System. Sci. Total Environ., 408, 3277-3291, 2010.

Parrella, J. P., Jacob, D. J., Liang, Q., Zhang, Y., Mickley, L. J., Miller, B., Evans, M. J., Yang, X., Pyle, J. A., Theys, N., and Van Roozendael, M.: Tropospheric bromine chemistry: implications for present and pre-industrial ozone and mercury, Atmos. Chem. Phys., 12, 6723-6740, 2012.

Peters, J.A.H.W. and Olivier, J.G.J.: EDGAR3/POET ENUSSUIBS; 1997 emissions and scenarios for 1995-2020; technical background information on global and regional sectoral emissions, Report no. 773301003, RIVM, Bilthoven, 2003.

Pirrone, N., Cinnirella, S., Feng, X., Finkelman, R. B., Friedli, H. R., Leaner, J., Mason, R., Mukherjee, A. B., Stracher, G. B., Streets, D. G., and Telmer, K.: Global mercury emissions to the atmosphere from anthropogenic and natural sources, Atmos. Chem. Phys., 10, 5951–5964, doi:10.5194/acp-10-5951-2010, 2010.

Platt, U. and Janssen, C.: Observation and role of the free radicals NO3, ClO, BrO and IO in the troposphere, Faraday Discuss., 100, 175?198, 1995.

Poissant, L., Pilote, M., Beauvais, C., Constant, P.,Zhang, H. H.: A year of continuous measurements of three atmospheric mercury species (GEM, RGM and Hgp) in southern Quebec, Canada, Atmos. Environ., 39, 1275-1287, doi:10.1016/j.atmosenv.2004.11.007, 2005.

Prestbo, E. M. and Gay, D. A.: Wet deposition of mercury in the U.S. and Canada, 1996-2005: Results and analysis of the NADP mercury deposition network (MDN), Atmospheric Environment, 43, 4223-4233, 2009.

Qureshi, A., Macleod, M., Sunderland, E., Hungerbühler, K.: Exchange of elemental mercury between the oceans and the atmosphere, in: Liu, G., Cai, Y. and N. O'Driscoll (Eds.), Environmental Chemistry and Toxicology of Mercury, John Wiley & Sons, Inc., Hoboken, NJ, USA, 389-421, doi: 10.1002/9781118146644.ch12, 2012.

Rutter, A. P., Shakya, K. M., Lehr, R., Schauer, J. J., Griffin, R. J.: Oxidation of gaseous elemental mercury in the presence of secondary organic aerosols. Atmospheric Environment 59, 86-92, 2012.

Sather, M. E., Mukerjee, S., Smith, L., Mathew, J., Jackson, C., Callison, R., Scrapper, L., Hathcoat, A., Adam, J., Keese, D., Ketcher, P., Brunette, R., Calstrom, J., and Van der Jagt, G.: Gaseous oxidized mercury dry deposition measurements in the Four Corners Area and Eastern Oklahoma, USA, Atmos. Pollut. Res., 4, 168-180, 2013.

Schroeder, W. H. and Munthe, J.: Atmospheric mercury – an overview, Atmos. Environ., 32, 809–822, 1998.

Seigneur, C., Karamchandani, P., Lohman, K., Vijayaraghavan, K., and Shia, R.-L.: Multiscale modeling of the atmospheric fate and transport of mercury, J. Geophys. Res., 106, 27795-27809, 2001.

Seigneur, C., Vijayaraghavan, K., and Lohman, K.: Atmospheric mercury chemistry: Sensitivity of global model simulations to chemical reactions, J. Geophys. Res., 111, D22306, doi:10.1029/2005JD006780, 2006.

Seigneur, C., and Lohman, K.: Effect of bromine chemistry on the atmospheric mercury cycle, J. Geophys. Res., 113, D23309, doi:10.1029/2008JD010262, 2008.

Selin, N. E. and Jacob, D. J.: Seasonal and spatial patterns of mercury wet deposition in the United States: Constraints on the contribution from North American anthropogenic sources, Atmos. Environ., 42, 5193-5204, doi:10.1016/j.atmosenv.2008.02.069, 2008.

Selin, N. E., Jacob, D. J., Yantosca, R. M., Strode, S., Jaeglé, L., and Sunderland, E. M.: Global 3-D land-ocean-atmosphere model for mercury: present-day versus preindustrial cycles and anthropogenic enrichment factors for deposition, Global biogeochemical cycles, 22, doi:10.1029/2007GB003040, 2008

Selin, N. E.: Global biogeochemical cycling of mercury: A review, Annu. Rev. Environ. Resour., 34, 43-63, 2009.

Shah, V., Jaeglé, L., Gratz, L. E., Ambrose, J. L., Jaffe, D. A., Selin, N. E., Song, S., Campos, T. L., Flocke, F. M., Reeves, M., Stechman, D., Stell, M., Festa, J., Stutz, J., Weinheimer, A. J., Knapp, D. J., Montzka, D. D., Tyndall, G. S., Apel, E. C., Hornbrook, R. S., Hills, A. J., Riemer, D. D., Blake, N. J., Cantrell, C. A., and Mauldin III, R. L.: Origin of oxidized mercury in the summertime free troposphere over the southeastern US. Atmos, Chem. Phys., 16, 1511-1530, doi:10.5194/acp-16-1511-2016, 2016.

Shetty, S. K., Lin, C.-J., Streets, D. G., Jang, C.: Model estimate of mercury emission from natural sources in East Asia, Atmos. Environ., 42, 8674-8685, 2008.

Sigler, J. M., Mao, H., and Talbot, R.: Gaseous elemental and reactive mercury in Southern New Hampshire, Atmos. Chem. Phys., 9, 1929-1942, doi:10.5194/acp-9-1929-2009, 2009.

Skamarock, W. C., Klemp, J. B., Dudhia, J., Gill, D. O., Barker, D. M., Wang, W., Powers, J. G.: A description of the Advanced Research WRF Version 2. NCAR/TN-468+STR.. NCAR Technical Note. Boulder, CO, USA, 2007.

Slemr, F., Angot, H., Dommergue, A., Magand, O., Barret, M., Weigelt, A., Ebinghaus, R., Brunke, E.-G., Pfaffhuber, K., Edwards, G., Howard D., Powell J., Keywood, M., and Wang, F.: Comparison of mercury concentrations measured at several sites in the Southern Hemisphere, Atmospheric Chemistry and Physics, 15, 3125–3133, doi:10.5194/acp-15-3125-2015, 2015.

Snider, G., Raofie, F., and Ariya, P. A. A.: Effects of relative humidity and CO(g) on the O3-initiated oxidation reaction of Hg0(g): Kinetic & product studies, Phys. Chem. Chem. Phys., 10, 5616-5623, doi:10.1039/B801226A, 2008.

Soerensen, A. L., Sunderland, E. M., Holmes, C. D., Jacob, D. J., Yantosca, R. M., Skov, H., Christensen, J. H., Strode, S. A., and Mason, R. P.: An improved global model for air-sea exchange of mercury: high concentrations over the north atlantic, Environmental Science and Technology, 44, 8574-8580, 2010.

Sommar, J., Gårdfeldt, K., Strömberg, D., and Feng, X.: A kinetic study of the gas-phase reaction between the hydroxyl radical and atomic mercury, Atmos. Environ., 35, 3049-3054, 2001.

Song, S., Selin, N. E., Soerensen, A. L., Angot, H., Artz, R., Brooks, S., Brunke, E.-G., Conley, G., Dommergue, A., Ebinghaus, R., Holsen, T. M., Jaffe, D. A., Kang, D., Kelley, P., Luke, W. T., Magand, O., Marumoto, K., Pfaffhuber, K. A., Ren, X., Sheu, G.-R., Slemr, F., Warneke, T., Weigelt, A., Weiss-Penzias, P., Wip, D. C., and Zhang, Q.: Top-down constraints on atmospheric mercury emissions and implications for global biogeochemical cycling, Atmos. Chem. Phys., 15, 7103-7125, 2015.

Sprovieri, F., Pirrone, N., Bencardino, M., D′Amore, F., Carbone, F., Cinnirella, S., Mannarino, V. , Landis, M., Ebinghaus, R., Weigelt, A., Brunke, E.-G., Labuschagne, C., Martin, L., Munthe, J., Wängberg, I., Artaxo, P., Morais, F., Cairns, W., Barbante, C., Diéguez, M. C., Garcia, P. E., Dommergue, A., Angot, H., Magand, O., Skov, H., Horvat, M., Kotnik, J., Read, K. A., Neves, L. M., Gawlik, B. M., Sena, F., Mashyanov, N., Obolkin, V. A., Wip, D., Feng, X., Zhang, H., Fu, X., Ramachandran, R., Cossa, D., Knoery, J., Marusczak, N., Nerentorp, M., and Norstrøm, C.: Atmospheric Mercury Concentrations observed at ground-based monitoring sites globally distributed in the framework of the GMOS network, Atmos. Chem. Phys. Discuss., doi:10.5194/acp-2016-466, 2016.

Sprovieri, F., Pirrone, N., Bencardino, M., D′Amore, F., Angot, H., Barbante, C., Brunke, E.-G., Arcega-Cabrera, F., Cairns, W., Comero, S., Diéguez, M. D. C., Dommergue, A., Ebinghaus, R., Feng, X. B., Fu, X., Garcia, P. E., Gawlik, B. M., Hageström, U., Hansson, K., Horvat, M., Kotnik, J., Labuschagne, C., Magand, O., Martin, L., Mashyanov, N., Mkololo, T., Munthe, J., Obolkin, V., Islas, M. R., Sena, F., Somerset, V., Spandow, P., Vardè, M., Walters, C., Wängberg, I., Weigelt, A., Yang, X., and Zhang, H.: Five-year records of Total Mercury Deposition flux at GMOS sites in the Northern and Southern Hemispheres, Atmos. Chem. Phys. Discuss., doi:10.5194/acp-2016-517, in review, 2016.

Steffen A., Lehnherr I., Cole A., Ariya P., Dastoor A., Durnford D., Kirk J., Pilote M.: Atmospheric mercury in the Canadian Arctic. Part I: A review of recent field measurements, Science of the Total Environment 509-510, 3-15, doi:10.1016/j.scitotenv.2014.10.109, 2015.

Subir, M., Ariya, P. A. and Dastoor, A. P.: A review of uncertainties in atmospheric modeling of mercury chemistry I. Uncertainties in existing kinetic parameters – Fundamental limitations and the importance of heterogeneous chemistry. Atmospheric Environment 45, 5664-5676, 2011.

Subir, M., Ariya, P. A., and Dastoor, A. P.: A review of the sources of uncertainties in atmospheric mercury modeling II. Mercury surface and heterogeneous chemistry – A missing link. Atmospheric Environment 46, 1-10, 2012.

Sunderland, E., Corbitt, E., Cossa, D., Evers, D., Friedli, H., Krabbenhoft, D., Levin, L., Pirrone, N., Rice, G.: Impacts of Intercontinental Mercury Transport on Human & Ecological Health, in: Pirrone, N. and T. Keating, Hemispheric Transport of Air Pollution 2010, Part B: Mercury, Air Pollution Studies No. 16. United Nations, 97-144, 2010.

Swartzendruber, P. and Jaffe, D.: Sources and Transport: A Global Issue, in: Bank M. S. (Ed.) Mercury in the environment, University of California Press, Berkeley and Los Angeles, California, 2012.

Tørseth, K., Aas, W., Breivik, K., Fjæraa, A. M., Fiebig, M., Hjellbrekke, A. G., Lund Myhre, C., Solberg, S., and Yttri, K. E.: Introduction to the European Monitoring and Evaluation Programme (EMEP) and observed atmospheric composition change during 1972–2009, Atmos. Chem. Phys., 12, 5447-5481, doi:10.5194/acp-12-5447-2012, 2012.

Tossell, J. A.: Calculation of the energetics for oxidation of gas-phase elemental Hg by Br and BrO, J. Phys. Chem. A, 107, 7804-7808, 2003.

Travnikov, O.: Contribution of the intercontinental atmospheric transport to mercury pollution in the Northern Hemisphere. Atmos. Environ. 39, 7541-7548, 2005.

Travnikov, O. and Ilyin, I.: The EMEP/MSC-E Mercury Modeling System, in: Pirrone, N. and Mason, R. P. (Eds.): Mercury Fate and Transport in the Global Atmosphere: Emissions, Measurements, and Models, Springer, pp. 571-587, 2009.

Travnikov, O., Jonson, J. E., Andersen, A. S., Gauss, M., Gusev A., Rozovskaya O., Simpson D., Sokovyh V., Valiyaveetil, S., and Wind, P.: Development of the EMEP global modelling framework: Progress report. EMEP/MSC-E Technical Report 7/2009, Meteorological Synthesizing Centre - East of EMEP, Moscow, 44 pp., available: http://www.msceast.org/index.php/publications/reports, 2009.

Travnikov, O., Lin C. J., Dastoor, A., Bullock, O. R., Hedgecock, I., Holmes, C., Ilyin, I., Jaegle, L., Jung, G., Pan, L., Pongprueksa, P., Ryzhkov, A., Seigneur, C., and Skov, H.: Global and Regional Modeling, in: Pirrone, N. and T. Keating, Hemispheric Transport of Air Pollution 2010, Part B: Mercury, Air Pollution Studies No. 16. United Nations, 97-144, 2010.

Travnikov, O.: Atmospheric transport of mercury, in: Liu, G., Cai, Y. and N. O'Driscoll (Eds.), Environmental Chemistry and Toxicology of Mercury, John Wiley & Sons, Inc., Hoboken, NJ, USA, 331-365, doi: 10.1002/9781118146644.ch10, 2012.

Van Loon, L., Mader, E., Scott, S. L.: Reduction of the aqueous mercuric ion by sulfite: UV spectrum of $HgSO_3$ and its intramolecular redox reaction. J. Phys. Chem. A, 104, 1621-1626, 2000.

Atmos. Chem. Phys. Discuss., doi:10.5194/acp-2016-924, 2016
Manuscript under review for journal Atmos. Chem. Phys.
Published: 31 October 2016

Atmospheric Chemistry and Physics
Discussions

Wang, X., Lin, C.-J., Feng, X.: Sensitivity analysis of an updated bidirectional air-surface exchange model for mercury vapor, Atmos. Chem. Phys., 14, 6273-6287, 2014.

Wang, X., Lin, C.-J., Yuan, W., Sommar, J., Zhu, W., and Feng, X.: Emission-dominated gas exchange of elemental mercury vapor over natural surfaces in China, Atmos. Chem. Phys., 16, 11125-11143, doi:10.5194/acp-16-11125-2016, 2016.

Weigelt, A., Temme, C., Bieber, E., Schwerin, A., Schuetze, M., Ebinghaus, R., and Kock H. H.: Measurements of atmospheric mercury species at a German rural background site from 2009 to 2011 - methods and results, Environ. Chem., 10, 102-110, doi:/10.1071/EN12107, 2013.

Weiss-Penzias, P., Amos, H. M., Selin, N. E., Gustin, M. S., Jaffe, D. A., Obrist, D., Sheu, G.-R., and Giang, A.: Use of a global model to understand speciated atmospheric mercury observations at five high-elevation sites, Atmos. Chem. Phys., 15, 1161-1173, doi:10.5194/acp-15-1161-2015, 2015.

Wesely, M. L.: Parameterization of surface resistances to gaseous dry deposition in regional-scale numerical models, Atmos. Environ., 23, 1293?1304, doi:10.1016/0004-6981(89)90153-4, 1989.

Wesely, M. L. and Hicks, B.B.: A review of the current status of knowledge on dry deposition. Atmos. Environ. 34, 2261-22, 2000.

Wright, G., Miller, M. B., Weiss-Penzias, P., and Gustin, M.: Investigation of mercury deposition and potential sources at six sites from the Pacific Coast to the Great Basin, USA, Sci. Total Environ, 470-471C, 1099-1113, doi:10.1016/j.scitotenv.2013.10.071, 2014.

Yang, X., Cox, R., Warwick, N., Pyle, J., Carver, G., O'Connor, F., Savage, N.: Tropospheric bromine chemistry and its impacts on ozone: A model study, J. Geophys. Res., 110, D23311, 2005.

Yang, X., Pyle, J. A., Cox, R. A., Theys, N., and Van Roozendael, M.: Snow-sourced bromine and its implications for polar tropospheric ozone, Atmos. Chem. Phys., 10, 7763-7773, doi:10.5194/acp-10-7763-2010, 2010.

Zhang, L.: A size-segregated particle dry deposition scheme for an atmospheric aerosol module, Atmos. Environ., 35, 549-560, doi:10.1016/S1352-2310(00)00326-5, 2001.

Zhang, L., Brook, J. R., and Vet, R.: A revised parameterization for gaseous dry deposition in air quality models, Atmos. Chem. Phys., 3, 1777-1804, doi:10.5194/acpd-3-1777-2003, 2003.

Zhang, L., Wright, L. P., Blanchard, P. A: Review of Current Knowledge Concerning Dry Deposition of Atmospheric Mercury, Atmos. Environ., 43, 5853-5864, 2009.

Zhang, Y., Jaeglé L., van Donkelaar, A., Martin, R. V., Holmes, C. D., Amos, H. M., Wang, Q., Jacob, D. J., Talbot, R., Artz, R., Holson, T. M., Felton, D., Miller, E. K., Perry, K. D., Schmeltz, D., Steffen, A., and Tordon, R.: Nested-grid simulation of mercury over North America, Atmos. Chem. Phys., 6095-6111, doi:10.5194/acp-12-6095-2012, 2012.

Atmos. Chem. Phys. Discuss., doi:10.5194/acp-2016-924, 2016
Manuscript under review for journal Atmos. Chem. Phys.
Published: 31 October 2016

Atmospheric Chemistry and Physics
Discussions

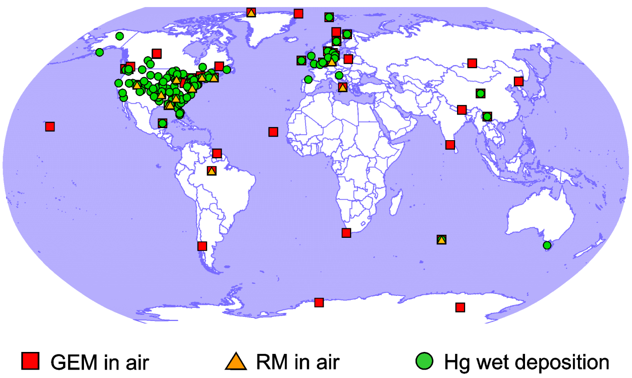

Figure 1. Location of measurement sites used in the study

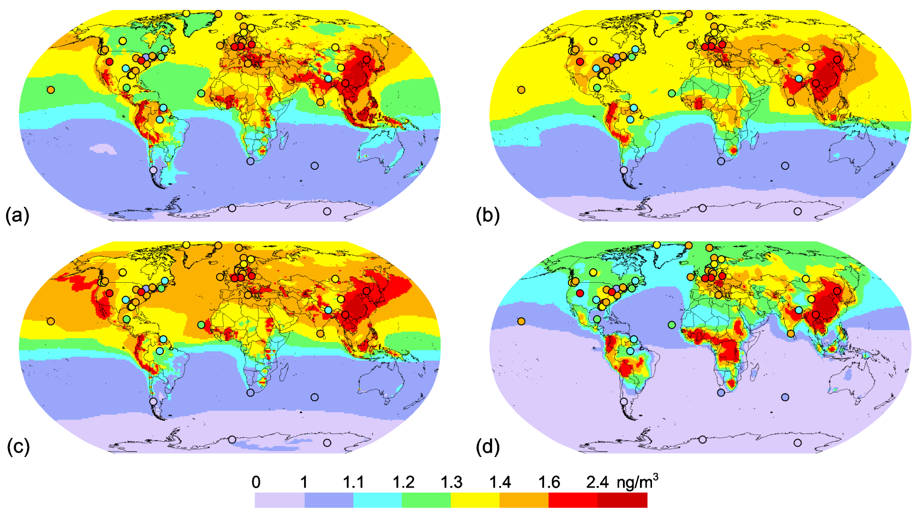

Figure 2. Spatial distribution of GEM air concentration in 2013 simulated according to the BASE case by four global models: (a) – GLEMOS; (b) – GEOS-Chem; (c) – GEM-MACH-Hg; (d) – ECHMERIT. Circles show observed values in the same colour scale.

Atmos. Chem. Phys. Discuss., doi:10.5194/acp-2016-924, 2016
Manuscript under review for journal Atmos. Chem. Phys.
Published: 31 October 2016

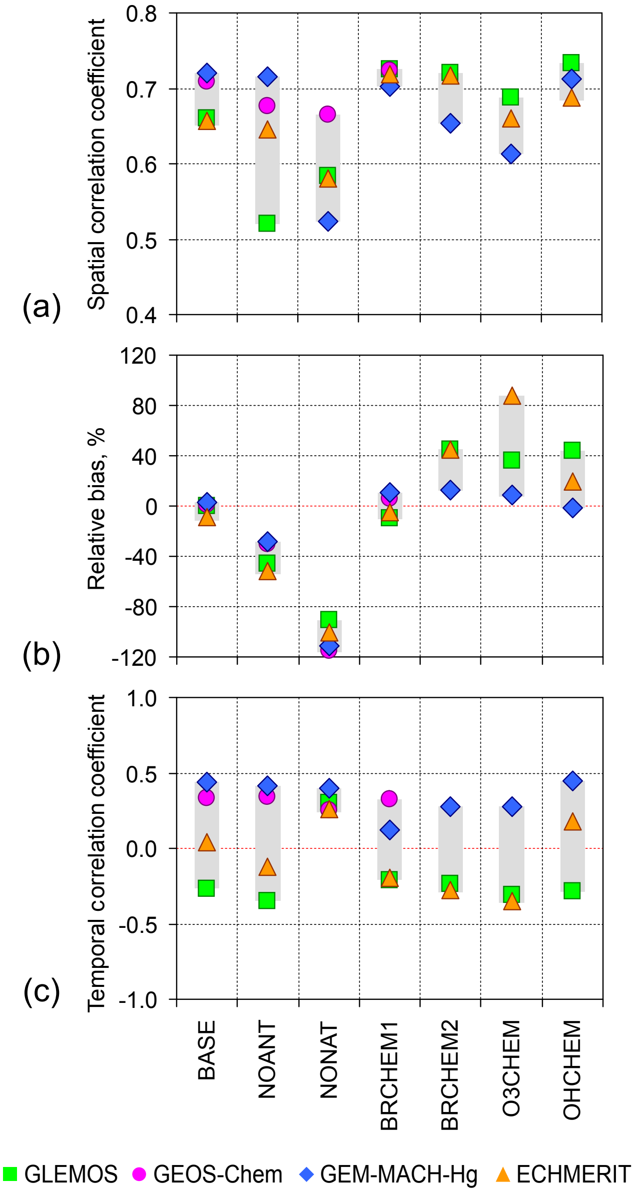

Figure 3. Spatial correlation coefficient (a), relative bias (b) and temporal correlation coefficient (c) of simulated and observed GEM air concentration for different model experiments.

Atmos. Chem. Phys. Discuss., doi:10.5194/acp-2016-924, 2016
Manuscript under review for journal Atmos. Chem. Phys.
Published: 31 October 2016

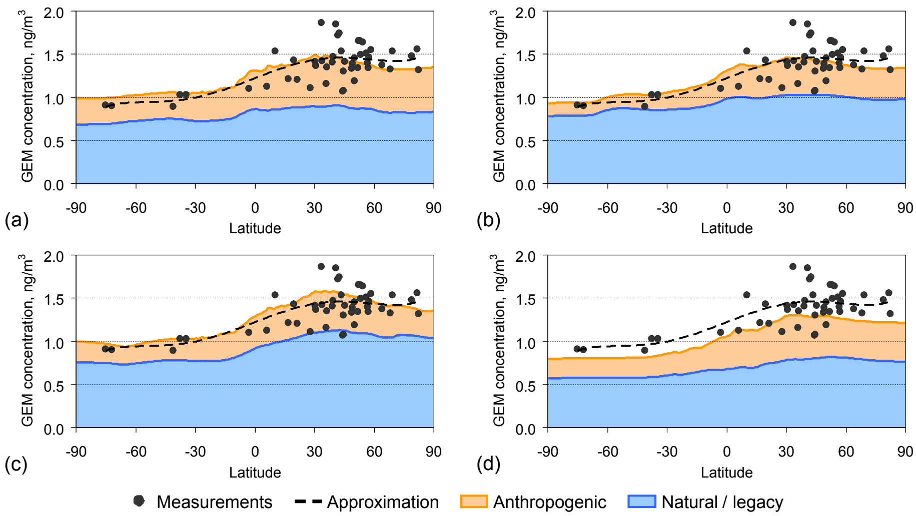

Figure 4. Global zonal-mean distribution of GEM air concentration in 2013 simulated by four models: (a) – GLEMOS; (b) – GEOS-Chem; (c) – GEM-MACH-Hg; (d) – ECHMERIT. Black dots are the same observations as in Fig. 2 and dotted line is a polynomial approximation

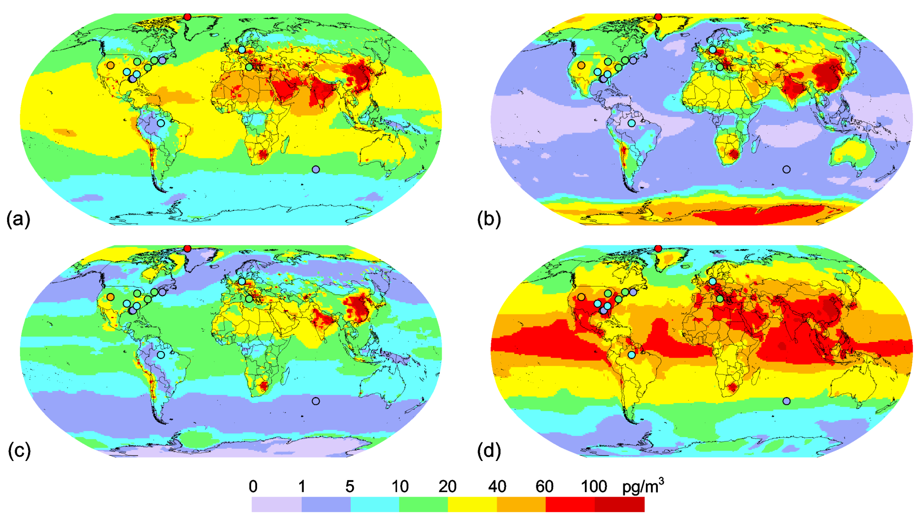

Figure 5. Spatial distribution of annual mean RM air concentration in 2013 simulated according to the BASE case by four global models: (a) – GLEMOS; (b) – GEOS-Chem; (c) – GEM-MACH-Hg; (d) – ECHMERIT. Circles show observed values in the same colour scale.

Atmos. Chem. Phys. Discuss., doi:10.5194/acp-2016-924, 2016
Manuscript under review for journal Atmos. Chem. Phys.
Published: 31 October 2016

Atmospheric Chemistry and Physics
Open Access
Discussions

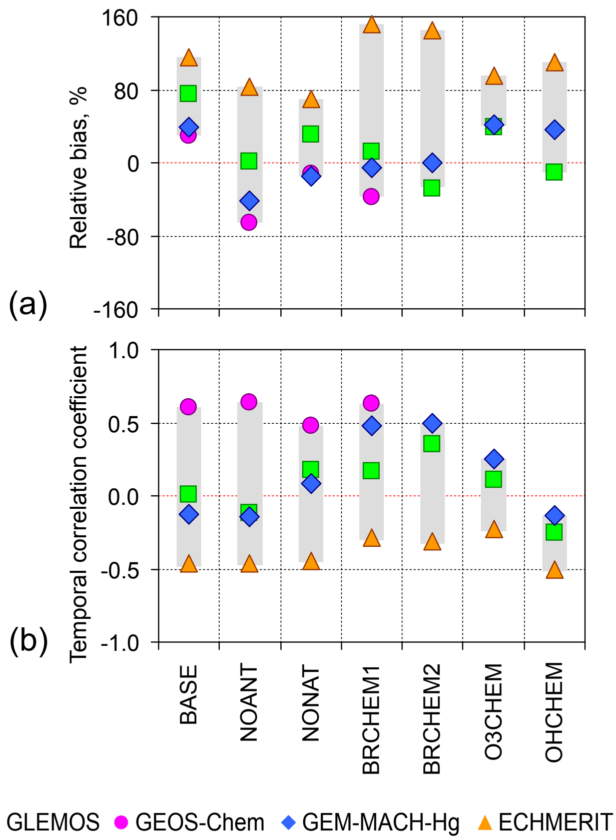

Figure 6. Relative bias (a) and spatial correlation coefficient (b) of simulated and observed annual mean RM air concentration for different model experiments.

Atmos. Chem. Phys. Discuss., doi:10.5194/acp-2016-924, 2016
Manuscript under review for journal Atmos. Chem. Phys.
Published: 31 October 2016

Atmospheric Chemistry and Physics
Open Access
Discussions

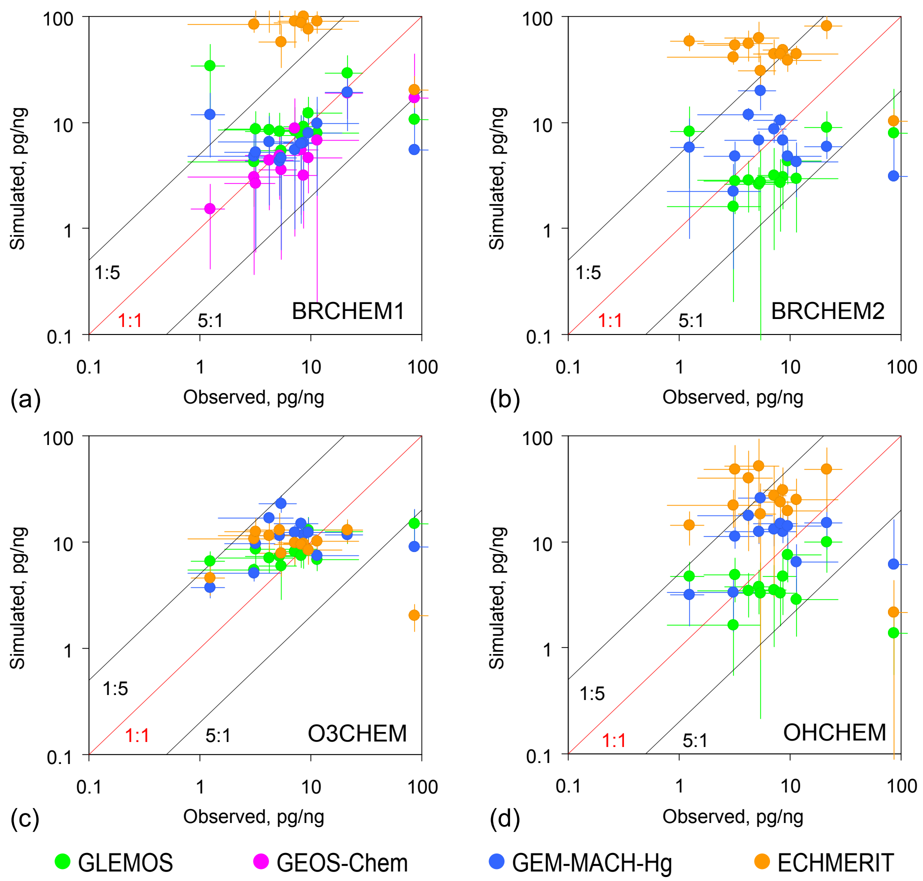

Figure 7. Scatter plots of simulated vs. observed ratios of annual mean RM concentration to GEM concentration in 2013 for different model experiments: (a) – BrCHEM1; (b) – BrCHEM2; (c) – O3CHEM; (d) – OHCHEM. Whiskers show standard deviation of monthly mean simulated and observed values. Dotted red line depicts the 1:1 ratio; dotted black lines show deviation by a factor of 5

Atmos. Chem. Phys. Discuss., doi:10.5194/acp-2016-924, 2016
Manuscript under review for journal Atmos. Chem. Phys.
Published: 31 October 2016

Atmospheric Chemistry and Physics Discussions
Open Access

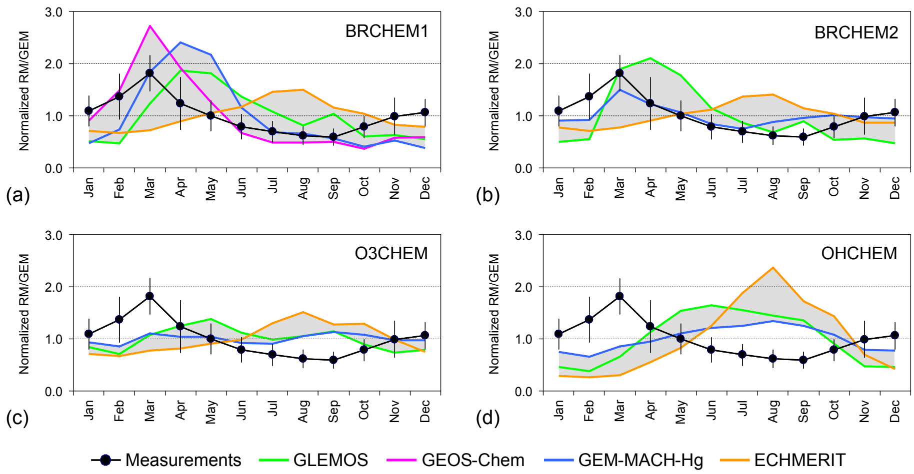

Figure 8. Normalized seasonal variation of monthly ratio of annual mean RM concentration to GEM concentration. Black line with dots shows observations averaged over selected sites (whiskers are standard deviation). Colored lines present model simulations averaged over the same cites for different model experiments: (a) – BrCHEM1; (b) – BrCHEM2; (c) – O3CHEM; (d) – OHCHEM

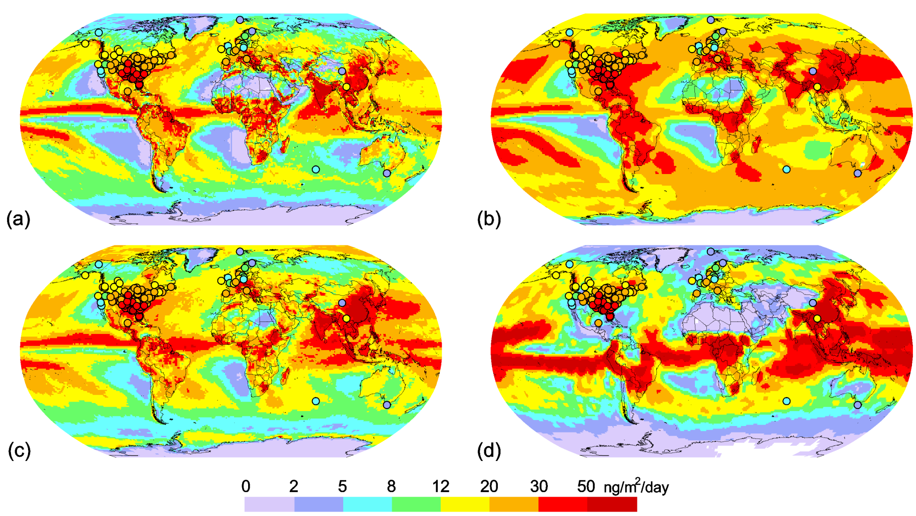

Figure 9. Spatial distribution of wet deposition flux in 2013 simulated according to the BASE case by four global models: (a) – GLEMOS; (b) – GEOS-Chem; (c) – GEM-MACH-Hg; (d) – ECHMERIT. Circles show observed values in the same colour scale.

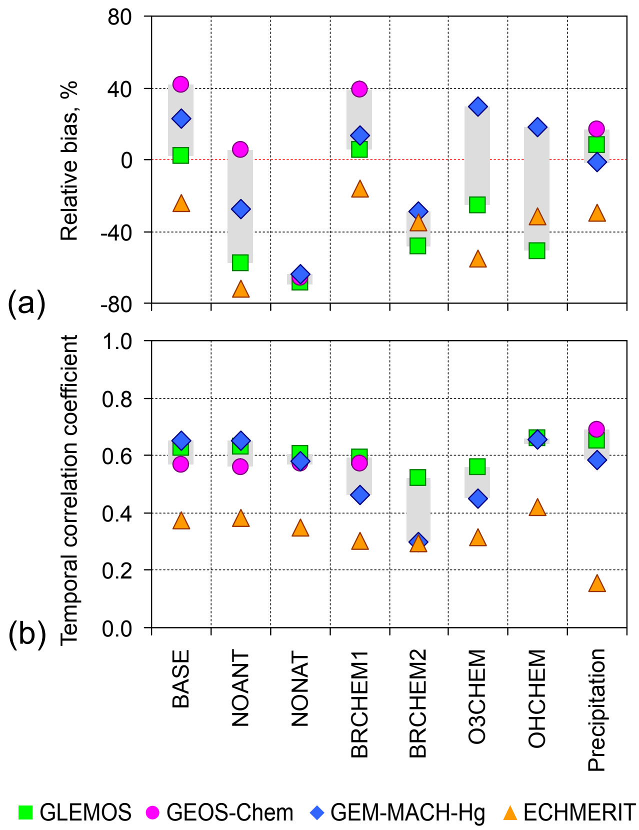

Figure 10. Relative bias (a) and spatial correlation coefficient (b) of simulated and observed annual mean wet deposition flux for different model experiments.

Atmos. Chem. Phys. Discuss., doi:10.5194/acp-2016-924, 2016
Manuscript under review for journal Atmos. Chem. Phys.
Published: 31 October 2016

Atmospheric Chemistry and Physics
Discussions
Open Access

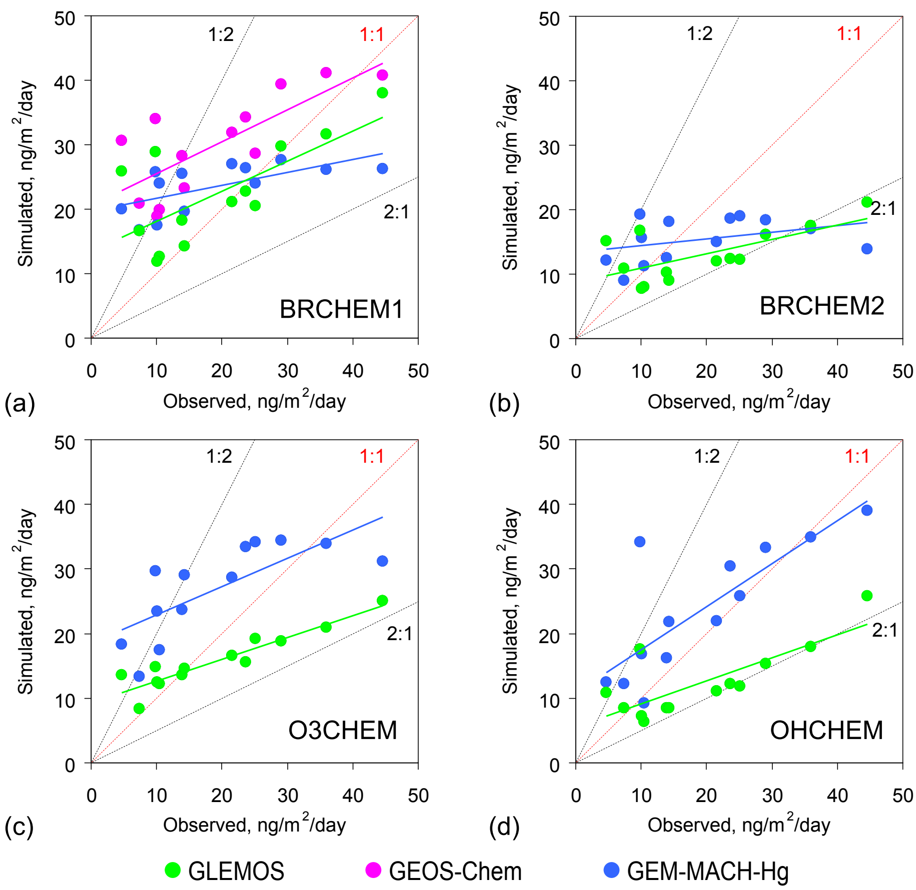

Figure 11. Scatter plots of simulated vs. observed annual mean wet deposition flux in 2013 averaged over different territorial groups of sites (see Table S3 in the Supplement) for different model experiments: (a) – BrCHEM1; (b) – BrCHEM2; (c) – O3CHEM; (d) – OHCHEM. Solid lines depict linear approximation. Dotted red line depicts the 1:1 ratio; dotted black lines show deviation by a factor of 2.

Atmos. Chem. Phys. Discuss., doi:10.5194/acp-2016-924, 2016
Manuscript under review for journal Atmos. Chem. Phys.
Published: 31 October 2016

Atmospheric Chemistry and Physics Discussions
Open Access

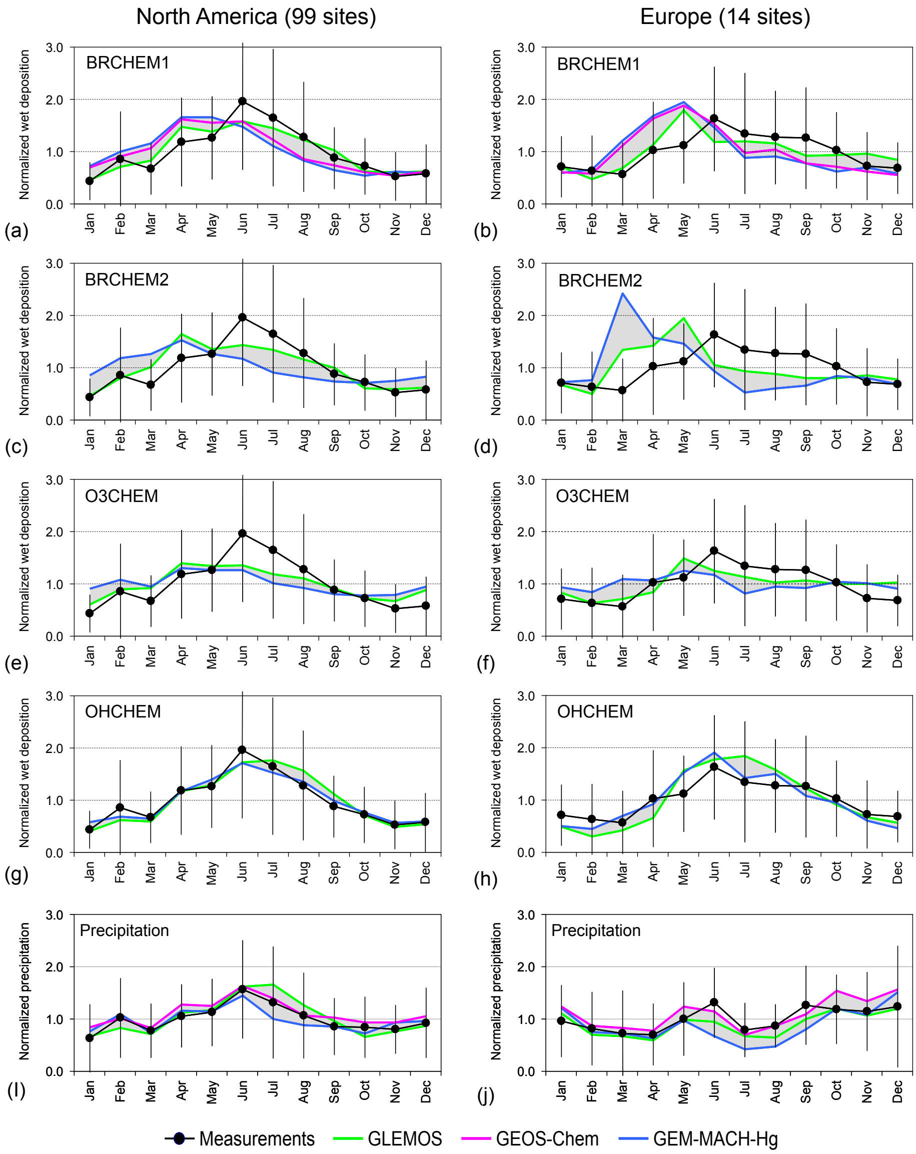

Figure 12. Normalized seasonal variation of monthly mean wet deposition flux in North America (left column) and Europe (right column). Black line with dots shows observations averaged over all sites in the regions (whiskers are standard deviation). Colored lines present model simulations averaged over the same sites for different model experiments: (a,b) – BrCHEM1; (c,d) – BrCHEM2; (e,f) – O3CHEM; (g,h) – OHCHEM. Seasonal variations of precipitation ammount in North America and Europe are also shown in panels (i) and (j), respectively.

Atmos. Chem. Phys. Discuss., doi:10.5194/acp-2016-924, 2016
Manuscript under review for journal Atmos. Chem. Phys.
Published: 31 October 2016

Table 1. Characteristics of the participating global chemistry transport models.

Model	GLEMOS	GEOS-Chem	GEM-MACH-Hg	ECHMERIT
Spatial resolution				
Horizontal	$1^\circ \times 1^\circ$	$2.5^\circ \times 2^\circ$	$1^\circ \times 1^\circ$	T42 ($\sim 2.8^\circ \times 2.8^\circ$)
Vertical	20 levels, top 10 hPa	47 levels, top 0.01 hPa	58 levels, top 7 hPa	19 levels, top 10 hPa
Driving meteorology				
Data support type	off-line	off-line	on-line	on-line
Meteorological driver	WRF / ECMWF	GEOS-FP	GEM	ECHAM5
Anthropogenic emission				
Global emission, t/y	1875	1875	1875	1875
Average speciation (base case)				
GEM : GOM : PBM	81 : 15 : 4	81 : 19 : 0[(a)]	96 : 3 : 1	81 : 15 : 4
Natural and re-emission				
Definition	prescribed / dynamic[(b)]	prescribed / dynamic[(c)]	prescribed / dynamic[(d)]	prescribed / dynamic[(e)]
Global emission, t/y (base case)	3995	5070	3660	8600
Gaseous chemistry (base-case reactions are in bold)				
Reaction rates[(f)], $cm^3\ molec^{-1}\ s^{-1}$				
$Hg^0 + Br \rightarrow HgBr$	3.7×10^{-13}[(g)]	$\mathbf{3.7 \times 10^{-13}}$[(g)]	3.7×10^{-13}[(g)]	3.7×10^{-13}[(g)]
$HgBr \rightarrow Hg^0 + Br$	$9.4 \times 10^{-2} s^{-1}$[(h)]	$\mathbf{9.4 \times 10^{-2}} s^{-1}$[(h)]	$1.7 \times 10^{-1} s^{-1}$[(i)]	$9.4 \times 10^{-2} s^{-1}$[(h)]
$HgBr + Br \rightarrow Hg^0 + Br_2$	3.9×10^{-11}[(j)]	$\mathbf{3.9 \times 10^{-11}}$[(j)]	—	—
$HgBr + Y \rightarrow HgBrY$, $Y = Br, OH$	2.5×10^{-10}[(k)]	$\mathbf{2.5 \times 10^{-10}}$[(k)]	2.5×10^{-10}[(k)]	2.5×10^{-10}[(k)]
$Hg^0 + O_3 \rightarrow Hg(II)$	$\mathbf{3.0 \times 10^{-20}}$[(l)]	—	3.0×10^{-20}[(l)]	$\mathbf{3.0 \times 10^{-20}}$[(l)]
$Hg^0 + OH \rightarrow Hg(II)$	$\mathbf{(0.9–8.7) \times 10^{-14}}$[(m)]	—	$\mathbf{3.0 \times 10^{-14}}$[(n)]	$\mathbf{8.7 \times 10^{-14}}$[(o)]
Aqueous chemistry (in cloud water)				
Oxidation agents	O_3, OH, $HOCl/OCl^-$	—	—	O_3, OH
Reduction agents	$SO_3^=$	—	—	—

Atmos. Chem. Phys. Discuss., doi:10.5194/acp-2016-924, 2016
Manuscript under review for journal Atmos. Chem. Phys.
Published: 31 October 2016

Atmospheric Chemistry and Physics
Open Access
Discussions

Table 1. Continued.

Model	GLEMOS	GEOS-Chem	GEM-MACH-Hg	ECHMERIT
Reference	Travnikov and Ilyin (2009); Travnikov et al. (2009)	Holmes et al. (2010); Amos et al. (2012); Song et al. (2015)	Durnford et al. (2012); Kos et al. (2013); Dastoor et al. (2015)	Jung et al. (2009); De Simone et al. (2014)

[(a)] Dynamic gas-partical partitioning of RM in the atmosphere according to Amos et al. (2012); [(b)] Prescribed fluxes from terrestrial and aquatic surfaces as a function of temperature and solar radiation, dynamic re-emission from snow; [(c)] Prescribed fluxes from terrestrial surfaces as a function of temperature and solar radiation, dynamic fluxes from aquatic surfaces based on multi-media modelling; [(d)] Prescribed fluxes from terrestrial surfaces as a function of solar radiation and leaf area index, dynamic re-emission from snow and aquatic surfaces; [(e)] Prescribed fluxes from terrestrial surfaces as a function of temperature and solar radiation, dynamically calculated ocean emissions; [(f)] Temperature and pressure dependence applied to most reactions, the reaction rates are given at 298 K and 1 atm; [(g)] Donohoue et al. (2006); [(h)] Goodsite et al. (2012); [(i)] Dibble et al. (2012); [(j)] Balabanov et al. (2005); [(k)] Goodsite et al. (2004); [(l)] Hall (1995); [(m)] Sommar et al. (2001) scaled down by a factor 0.1 in the cloud environment and below clouds to account for reduction of photochemical activity (Seigneur et al., 2001); [(n)] Sommar et al. (2001) scaled down by a factor 0.34 to take into account possible dissociation/reduction reactions; [(o)] Sommar et al. (2001); [(p)] Parrella et al. (2012); [(q)] Yang et al. (2005, 2010); [(r)] Emmons et al. (2010).

Table 2. Specifications of model experiments.

Code	Anthropogenic emissions	Gas-phase chemistry	Comment
BASE	UNEP2010[(a)]	Model standard configuration	Base run
NoANT	No emission	Model standard configuration	Effect of anthropogenic emissions
NoNAT[(b)]	—	—	Effect of natural/secondary emissions
BrCHEM1	UNEP2010, all emissions as GEM[(c)]	GEM oxidation by Br	Br dataset from GEOS-Chem[(d)]
BrCHEM2	UNEP2010, all emissions as GEM	GEM oxidation by Br	Br dataset from p-TOMCAT[(e)]
O3CHEM	UNEP2010, all emissions as GEM	GEM oxidation by O_3	O_3 dataset from MOZART[(f)]
OHCHEM	UNEP2010, all emissions as GEM	GEM oxidation by OH	OH dataset from MOZART[(f)]

[(a)] AMAP/UNEP (2013b); [(b)] Virtual experiment obtained by subtraction of NoANT results from the BASE case; [(c)] All GOM and PBM emissions summed to GEM to keep constant total Hg emissions; [(d)] Parrella et al. (2012); [(e)] Yang et al. (2005, 2010); [(f)] Emmons et al. (2010).